Global Analysis of TSSAs: Transversity, Nucleon Tensor Charges, and Opportunities for SoLID

Daniel Pitonyak
Lebanon Valley College, Annville, PA, USA

SoLID Workshop
June 18, 2024

$$S_T^i \, h_1^q(x) = \frac{1}{2}\int \frac{d\xi^-}{2\pi} e^{ixP^+\xi^-} \mathrm{Tr}[\langle P,S|\bar{\psi}_q(0)\mathcal{W}(0,\xi^-)\psi_q(\xi^-)i\sigma^{i+}\gamma_5|P,S\rangle]$$

transversity PDF - universal parton density that quantifies the degree of transverse polarization of quarks within a transversely polarized nucleon

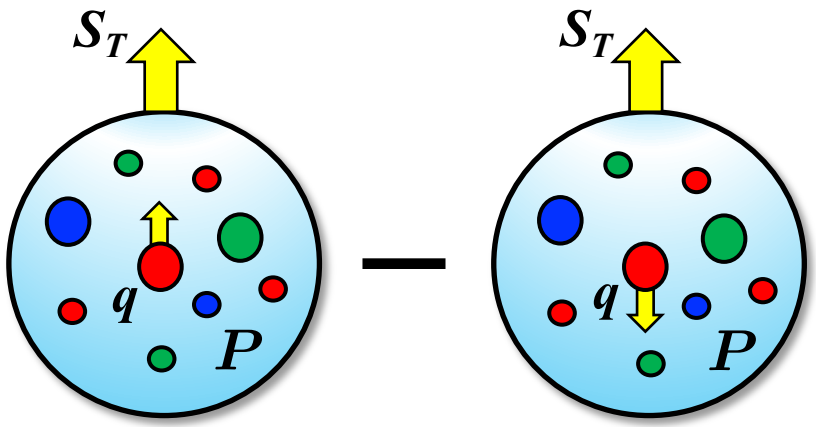

$$\delta q \equiv \int_0^1 dx\,[h_1^q(x) - h_1^{\bar{q}}(x)]$$

tensor charge for an individual flavor

$$g_T \equiv \delta u - \delta d$$

isovector combination

$$\langle P|\bar{\psi}_q \sigma^{i+} \psi_q|P\rangle = \boldsymbol{\delta q}\,[\bar{u}_P \sigma^{i+} u_P]$$

local matrix element - can be computed in lattice QCD as well as other approaches like Dyson-Schwinger equations and several other models

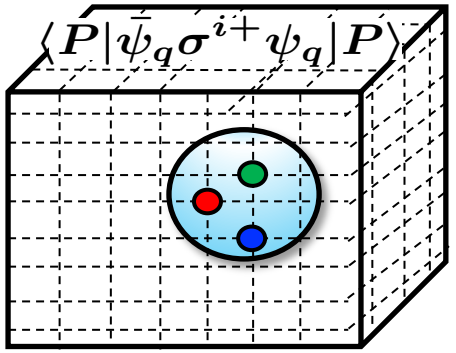

$[J^{(3)}_{nn'}(Q)]^{\delta\delta'}_{\mu\nu} =$

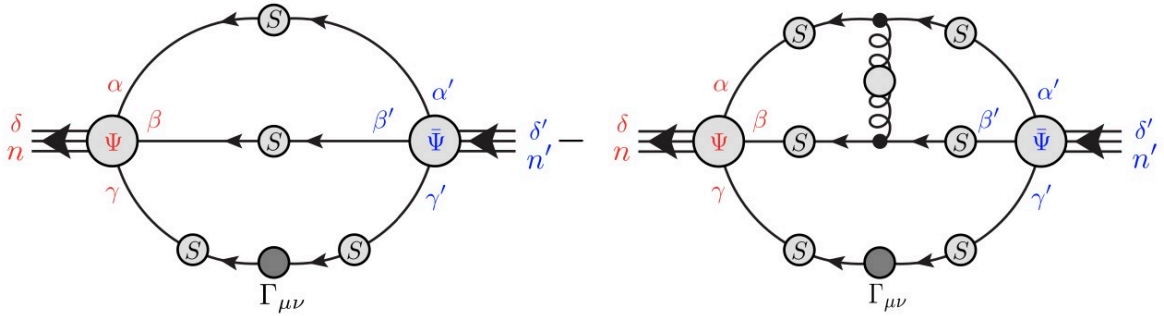

From Wang, et al. (2018)

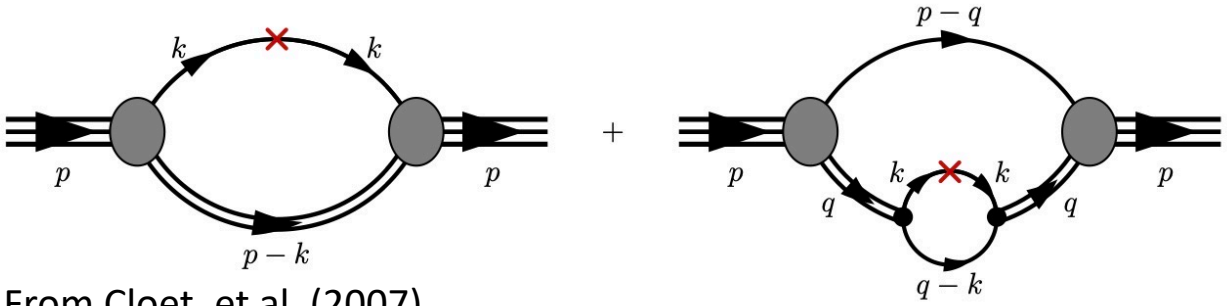

From Cloet, et al. (2007)

- Importance of the nucleon tensor charge:
  - Like the scalar, vector, and axial charges, it is a fundamental charge of the nucleon (although scale dependent)
  - Since helicity PDF ≠ transversity PDF in relativistic quantum mechanics, it can be considered a measure of relativistic effects in the nucleon
  - Key point of comparison between QCD phenomenology/experiment and lattice QCD as well as model calculations
  - Needed in certain beyond the Standard Model studies (e.g., beta decay, EDM)

$$\mathcal{L}_{n\to pe\bar{\nu}_e} \sim \ldots + 4\sqrt{2}G_F V_{ud}\, \boldsymbol{g_T}\epsilon_T\, \bar{p}\,\sigma^{\mu\nu} n\, \bar{e}\,\sigma_{\mu\nu}\nu_e + \ldots$$

Lagrangian for neutron beta decay

BSM coupling

$$\tilde{d}_p = \tilde{d}_u\, \boldsymbol{\delta u} + \tilde{d}_d\, \boldsymbol{\delta d}$$

proton EDM

quark EDMs

- Model calculations have provided valuable insight into the behavior of $h_1(x)$ we should expect from phenomenology

From the "TMD Handbook" – Pasquini, et al. (2008) - LFCQM; Jakob, et al. (1997) - spectator; Avakian, et al. (2010) - bag model

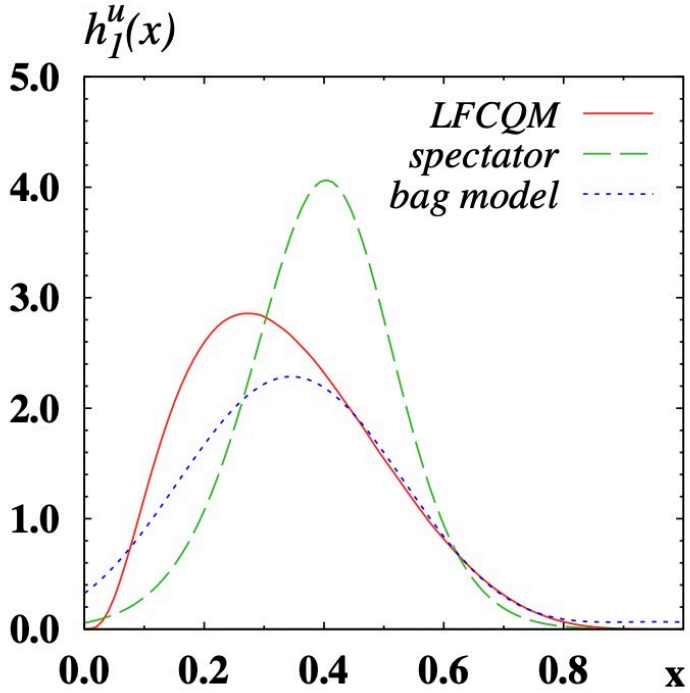

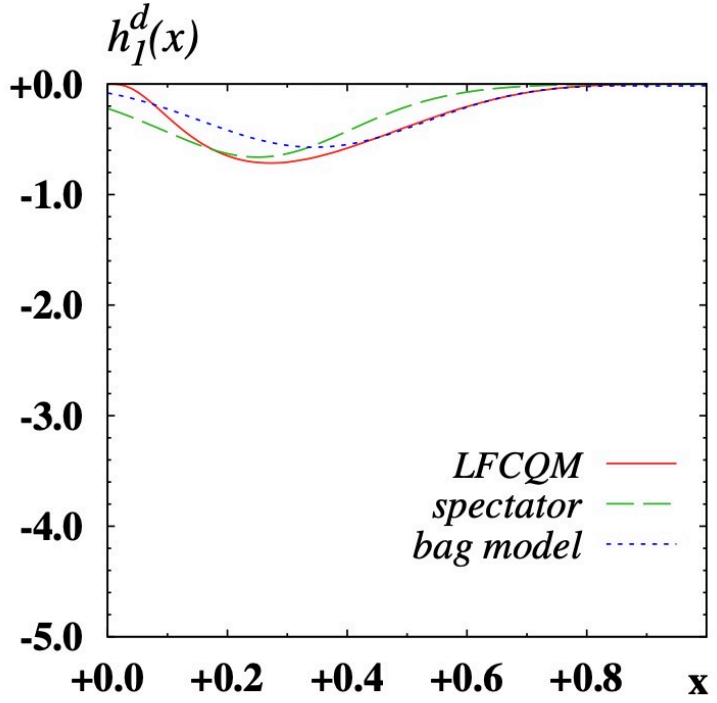

- Lattice QCD also has the ability now to compute $h_1(x)$

Alexandrou, et al. (2019)

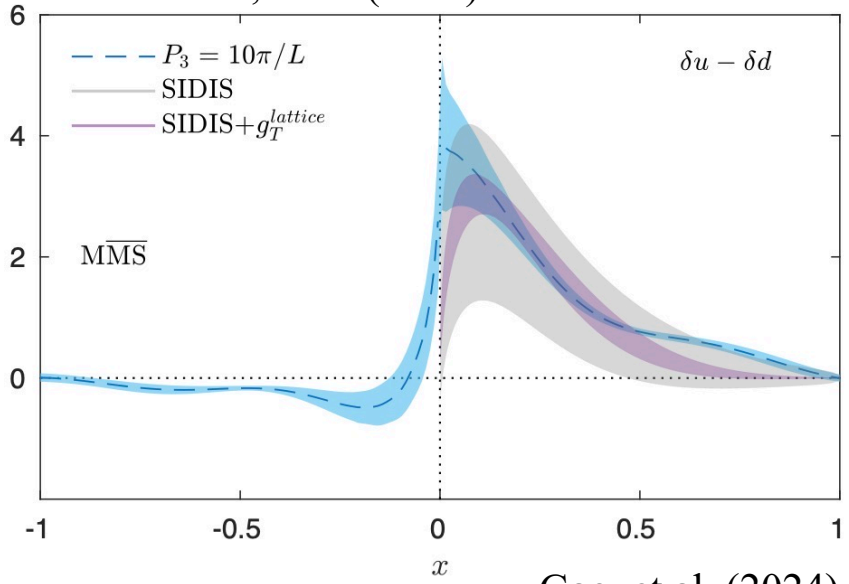

Egerer, et al. (2021)

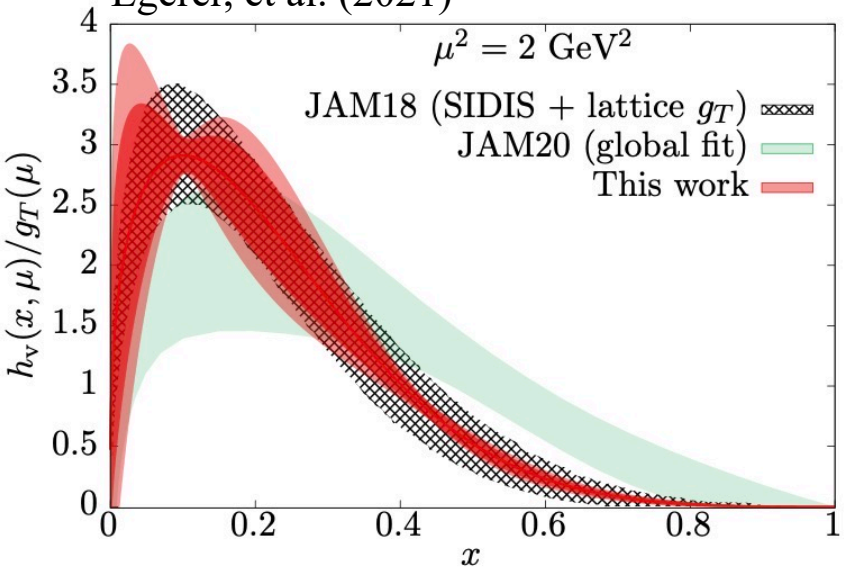

Gao, et al. (2024)

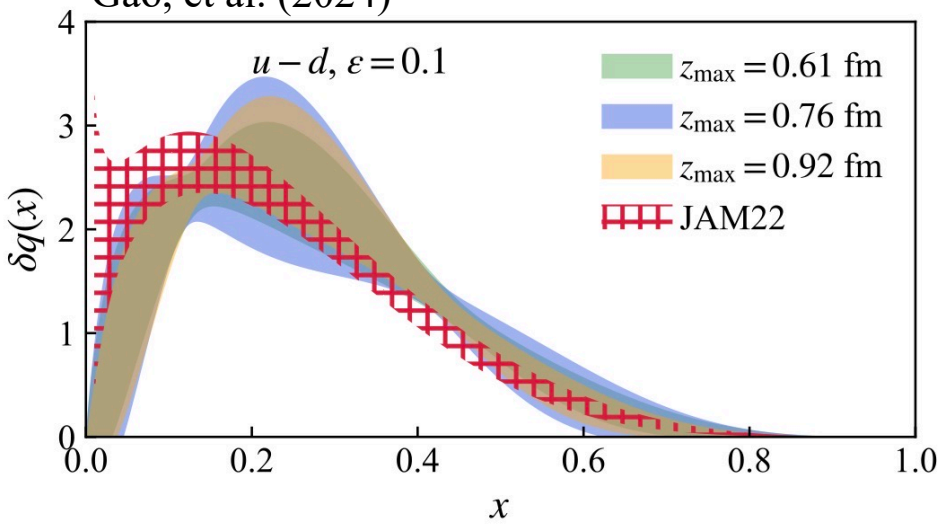

Anselmino, et al. (2007, 2009, 2013, 2015);
Goldstein, et al. (2014); Kang, et al. (2016); Radici, et al. (2013, 2015, 2018);
Benel, et al. (2020); D'Alesio, et al. (2020); Cammarota, et al. (2020);
Gamberg, et al. (2022); Cocuzza, et al. (2024); Boglione, et al. (2024)

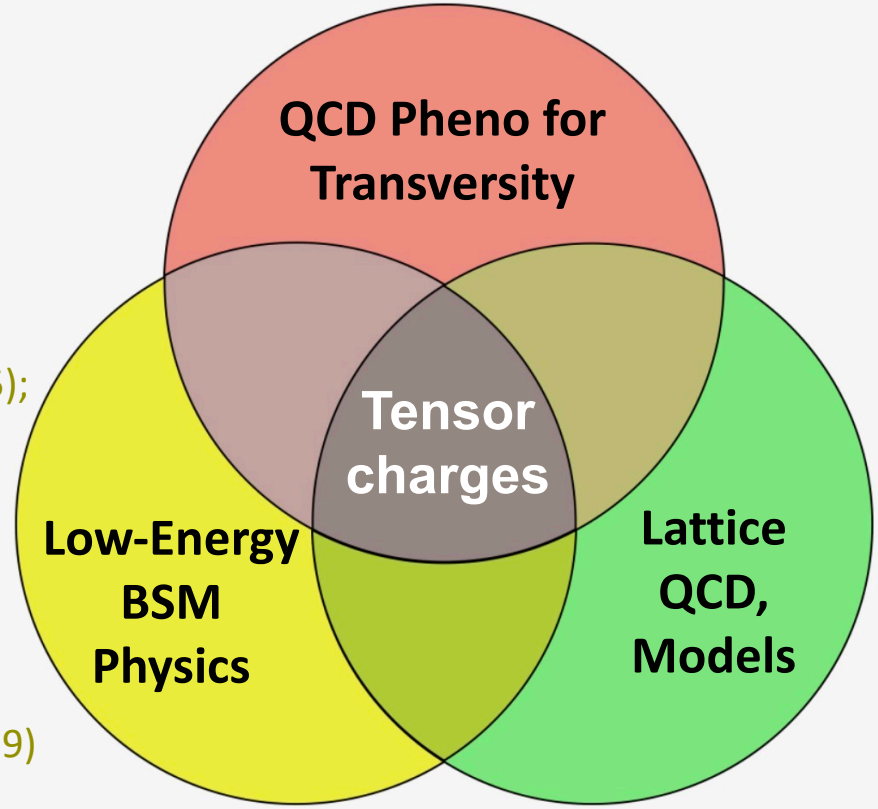

Herczeg (2001);
Erler, Ramsey-Musolf (2005);
Pospelov, Ritz (2005);
Severijns, et al. (2006);
Cirigliano, et al. (2013);
Courtoy, et al. (2015);
Yamanaka, et al. (2017);
Liu, et al. (2018);
Gonzalez-Alonso, et al. (2019)

He, Ji (1995);
Barone, et al. (1997);
Schweitzer, et al. (2001);
Gamberg, Goldstein (2001);
Pasquini, et al. (2005);
Wakamatsu (2007);
Cloet, et al. (2007);
Lorce (2009);
Gupta, et al. (2018);
Yamanaka, et al. (2018);
Hasan, et al. (2019);
Alexandrou, et al. (2019, 2023);
Yamanaka, et al. (2013);
Pitschmann, et al. (2015);
Xu, et al. (2015);
Wang, et al. (2018);
Liu, et al. (2019);
Gao, et al. (2023)

Lebanon Valley College

D. Pitonyak

Updated QCD Global Analysis of TSSAs for Single-Hadron Fragmentation

Gamberg, Malda, Miller, DP, Prokudin, Sato, Phys. Rev. D **106**, 034014 (2022)

User-friendly jupyter notebook to calculate functions and asymmetries:
https://colab.research.google.com/github/pitonyak25/jam3d_dev_lib/blob/main/JAM3D_Library.ipynb

LHAPDF tables available (thanks to C. Cocuzza):
https://github.com/pitonyak25/jam3d_dev_lib/tree/main/LHAPDF_tables

Jefferson Lab Angular Momentum Collaboration

$$\ell p^{\uparrow} \to \ell h X$$

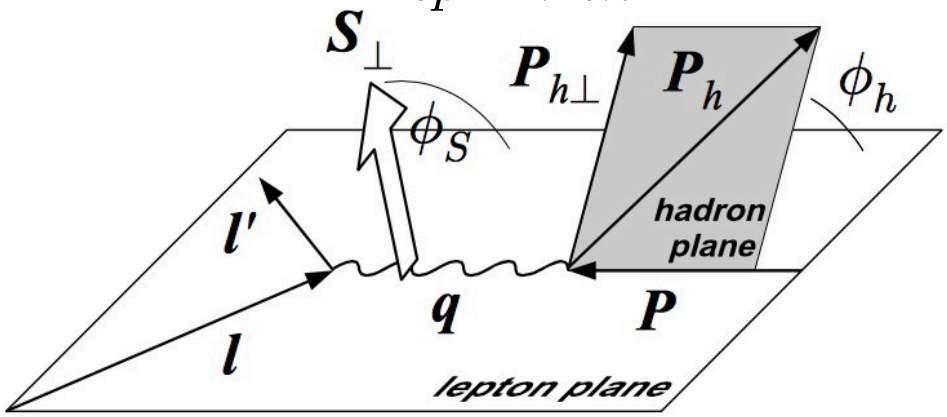

$$\{\pi, p\}p^{\uparrow} \to \{\ell^+\ell^-, W^{\pm}, Z\}X$$

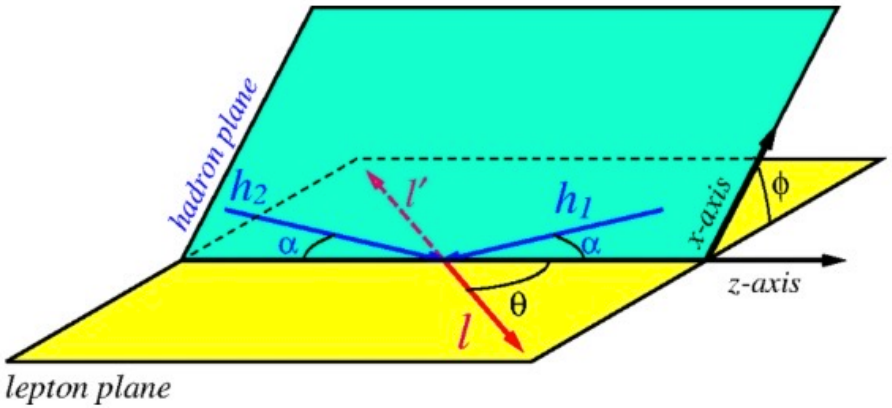

$$F_{UT}^{\sin(\phi_h-\phi_S)} = \mathcal{C}\left[-\frac{\hat{h}\cdot\vec{k}_T}{M} f_{1T}^{\perp} D_1\right]$$

$$F_{TU}^{\sin\phi} = \mathcal{C}\left[-\frac{\hat{h}\cdot\vec{k}_{aT}}{M_a} f_{1T}^{\perp} \bar{f}_1\right]$$

TMD/Collins-Soper-Sterman (CSS) Evolution

OPE

Sudakov exponentials (gluon radiation)

$$\tilde{f}_{1T}^{\perp(1)}(x, b_T; Q^2, \mu_Q) \sim F_{FT}(x, x; \mu_{b_*}) \exp\left[-S_{pert}(b_*(b_T); \mu_{b_*}, Q, \mu_Q) - S_{NP}^{f_{1T}^{\perp}}(b_T, Q)\right]$$

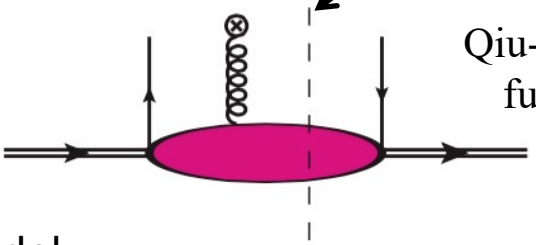

Qiu-Sterman function

$$g_{f_{1T}^{\perp}}(x, b_T) + g_K(b_T)\ln(Q/Q_0)$$

(Aybat, et al. (2012); Bury, et al. (2021); Echevarria, et al. (2014, 2021))

Parton model

$$\pi F_{FT}(x,x) = \int d^2\vec{k}_T \frac{k_T^2}{2M^2} f_{1T}^{\perp}(x, k_T^2) \equiv f_{1T}^{\perp(1)}(x)$$

(Boer, Mulders, Pijlman (2003), see also del Rio, et al. (2024))

$\ell N^{\uparrow} \to \ell h X$

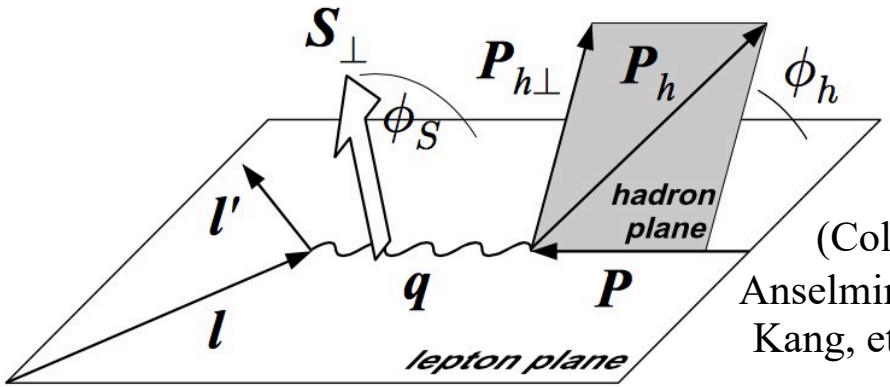

(Collins (1992); Anselmino, et al. (2007); Kang, et al. (2016); …)

$e^+e^- \to h_1 h_2 X$

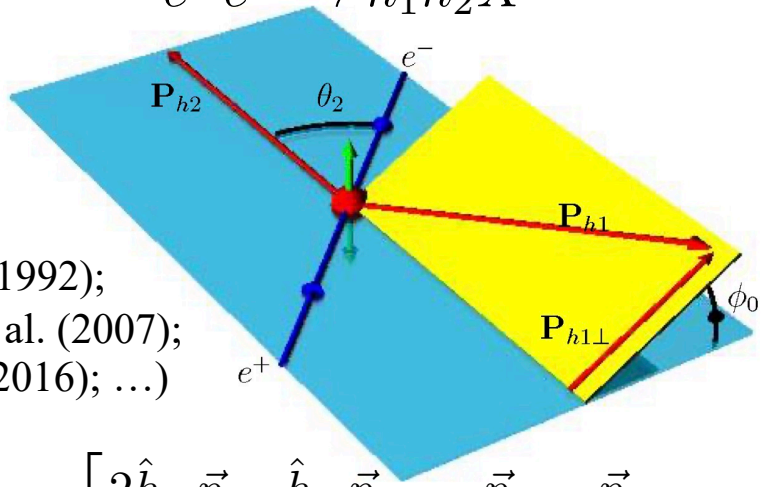

$$F_{UT}^{\sin(\phi_h+\phi_S)} = \mathcal{C}\left[-\frac{\hat{h}\cdot\vec{p}_\perp}{M_h} h_1 H_1^\perp\right] \qquad F_{UU}^{\cos(2\phi_0)} = \mathcal{C}\left[\frac{2\hat{h}\cdot\vec{p}_{a\perp}\,\hat{h}\cdot\vec{p}_{b\perp} - \vec{p}_{a\perp}\cdot\vec{p}_{b\perp}}{M_a M_b} H_1^\perp \bar{H}_1^\perp\right]$$

TMD/Collins-Soper-Sterman (CSS) Evolution

OPE — Sudakov exponentials (gluon radiation)

$$\tilde{h}_1(x, b_T; Q^2, \mu_Q) \sim h_1(x; \mu_{b_*}) \exp\left[-S_{pert}(b_*(b_T); \mu_{b_*}, Q, \mu_Q) - S_{NP}^{h_1}(b_T, Q)\right]$$

$$\tilde{H}_1^{\perp(1)}(z, b_T; Q^2, \mu_Q) \sim H_1^{\perp(1)}(z; \mu_{b_*}) \exp\left[-S_{pert}(b_*(b_T); \mu_{b_*}, Q, \mu_Q) - S_{NP}^{H_1^\perp}(b_T, Q)\right]$$

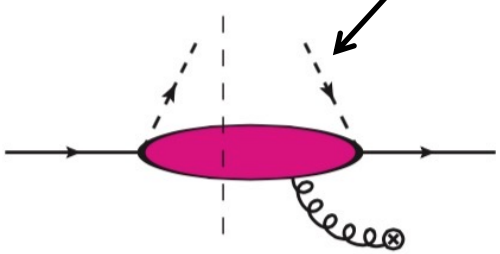

qgq fragmentation function

Parton model

$$h_1(x) = \int d^2\vec{k}_T\, h_1(x, \vec{k}_T^2)$$

$$H_1^{\perp(1)}(z) = z^2 \int d^2\vec{p}_\perp \frac{p_\perp^2}{2M_h^2} H_1^\perp(z, z^2 p_\perp^2)$$

$p^{\uparrow}p \to hX$

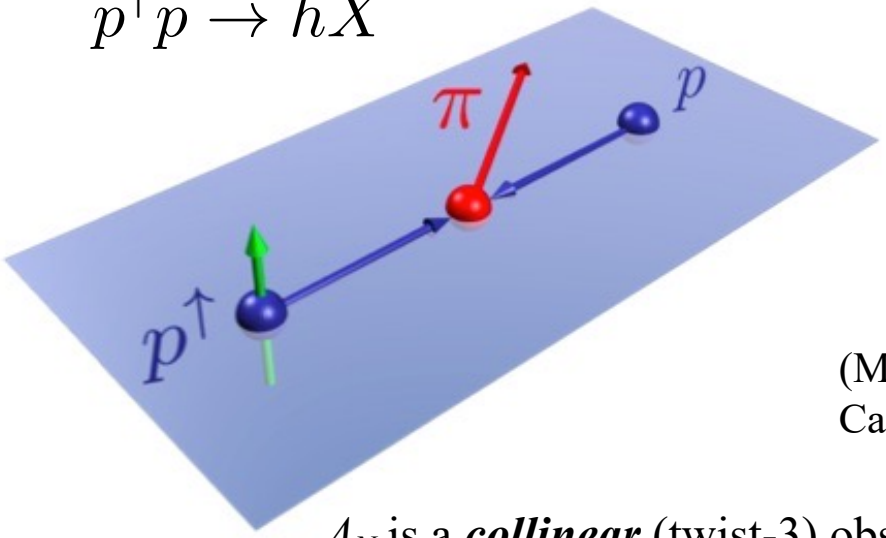

$$d\Delta\sigma(S_T) \sim \underbrace{H_{QS} \otimes f_1 \otimes \boldsymbol{F_{FT}} \otimes D_1}_{\text{Qiu-Sterman term}} + \underbrace{H_F \otimes f_1 \otimes \boldsymbol{h_1} \otimes \left(\boldsymbol{H_1^{\perp(1)}}, \tilde{\boldsymbol{H}}\right)}_{\text{Fragmentation term}}$$

(Metz, DP (2012); Kanazawa, et al. (2014); Cammarota, et al. (2020); Gamberg, et al. (2017, 2022))

A_N is a ***collinear*** (twist-3) observable

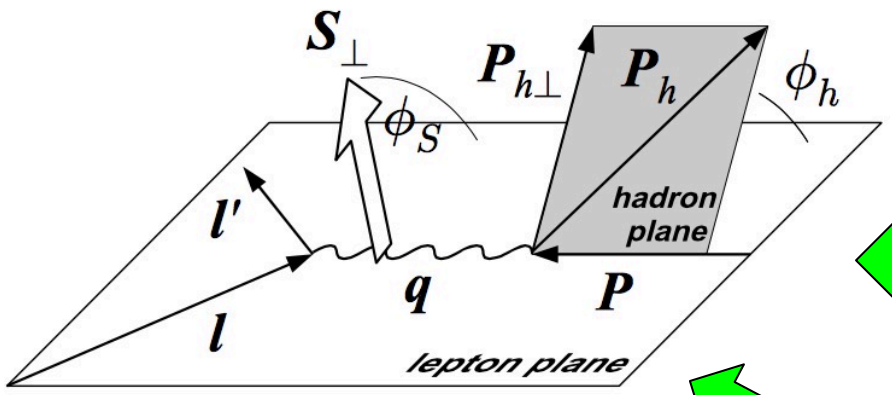

$h_1,\ F_{FT},\ H_1^{\perp(1)},\ \tilde{H}$

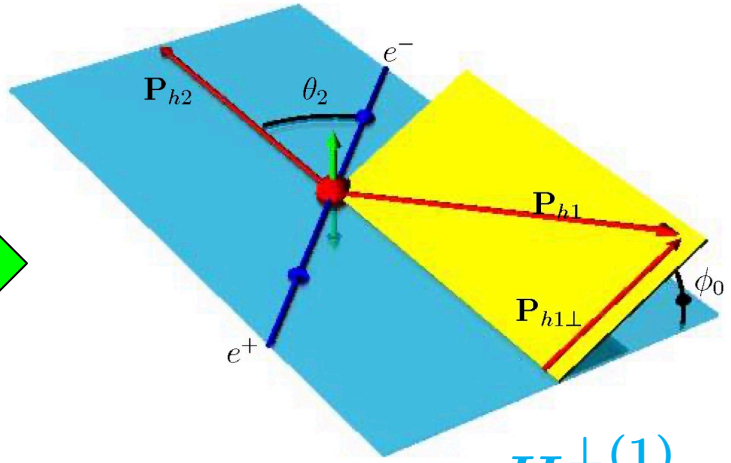

$H_1^{\perp(1)}$

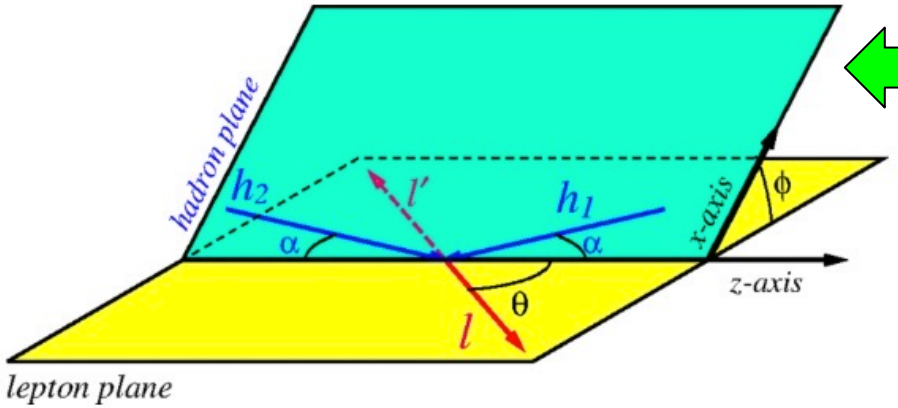

F_{FT}

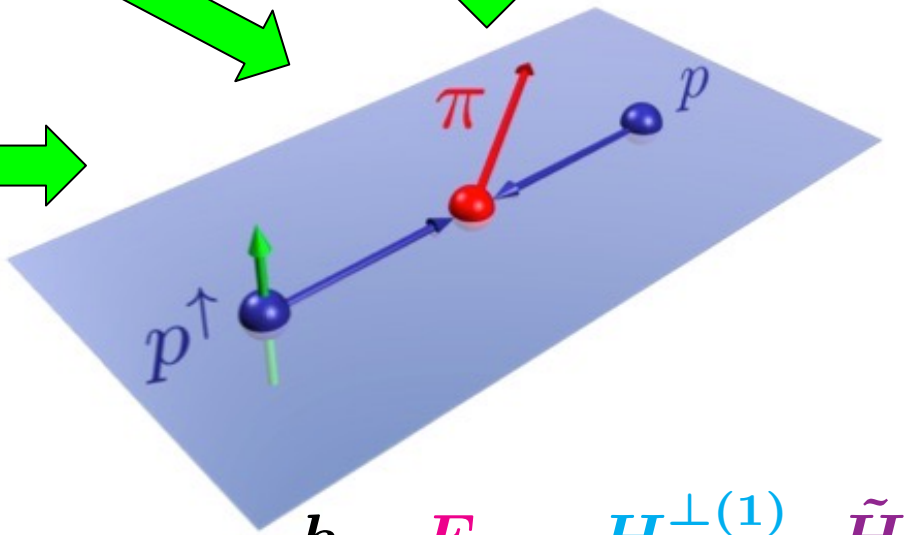

$h_1,\ F_{FT},\ H_1^{\perp(1)},\ \tilde{H}$

- Analyze TSSAs in SIDIS, Drell-Yan, e^+e^- annihilation, and proton-proton collisions and extract

$$h_1(x),\ F_{FT}(x,x),\ H_1^{\perp(1)}(z),\ \tilde{H}(z)$$

along with the relevant transverse momentum widths for the Sivers, transversity, and Collins functions: $\langle k_T^2\rangle_{f_{1T}^\perp}, \langle k_T^2\rangle_{h_1}, \langle p_\perp^2\rangle_{H_1^\perp}^{fav}, \langle p_\perp^2\rangle_{H_1^\perp}^{unf}$

- We use a Gaussian ansatz: $F^q(x,k_T^2) \sim F^q(x)e^{-k_T^2/\langle k_T^2\rangle}$ where

$$F^q(x) = \frac{N_q\, x^{a_q}(1-x)^{b_q}(1+\gamma_q\, x^{\alpha_q}(1-x)^{\beta_q})}{\mathrm{B}[a_q+2, b_q+1] + \gamma_q \mathrm{B}[a_q+\alpha_q+2, b_q+\beta_q+1]}$$

NB. $\{\gamma, \alpha, \beta\}$ only used for $H_1^{\perp(1)}(x)$, $b_u = b_d$ for $h_1(x), f_{1T}^{\perp(1)}(x)$

- DGLAP-type evolution for the collinear functions analogous to Duke & Owens (1984): double-log Q^2-dependent term explicitly added to the parameters

- Additional data/constraints included in the fit compared to 2020:
  - Collins and Sivers effects (3D-binned) SIDIS data from HERMES (2020)
  - $A_{UT}^{\sin\phi_S}$ data (x and z projections only) from HERMES (2020)

$$\int d^2\vec{P}_{hT}\, F_{UT}^{\sin\phi_S} = -\frac{x}{z}\sum_q e_q^2 \frac{2M_h}{Q} h_1^{q/N}(x)\,\tilde{H}^{h/q}(z)$$

  - Lattice data on g_T at the physical pion mass from ETMC (Alexandrou, et al. (2019))

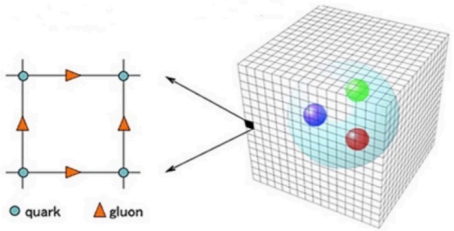

  - Imposing the Soffer bound on transversity: $|h_1^q(x)| \leq \frac{1}{2}(f_1^q(x) + g_1^q(x))$

Generate "data" (central value and 1-σ uncertainty) using recent simultaneous fit of f_1 and g_1 from Cocuzza, et al. (2022) and add to the χ^2 if SB is violated by more than the uncertainty in the data

$$\chi^2/N_{\text{pts.}} = 647/634 = 1.02$$

Observable	Reactions	Non-Perturbative Function(s)	χ^2/npts
$A_{UT}^{\sin(\phi_h-\phi_S)}$	$e+(p,d)^\uparrow \to e+(\pi^+,\pi^-,\pi^0)+X$	$f_{1T}^\perp(x,\vec{k}_T^2)$	$182.9/166 = 1.10$
$A_{UT}^{\sin(\phi_h+\phi_S)}$	$e+(p,d)^\uparrow \to e+(\pi^+,\pi^-,\pi^0)+X$	$h_1(x,\vec{k}_T^2), H_1^\perp(z,z^2\vec{p}_T^2)$	$181.0/166 = 1.09$
${}^*A_{UT}^{\sin\phi_S}$	$e+p^\uparrow \to e+(\pi^+,\pi^-,\pi^0)+X$	$h_1(x), \tilde{H}(z)$	$18.6/36 = 0.52$
$A_{UC/UL}$	$e^+ + e^- \to \pi^+\pi^-(UC,UL)+X$	$H_1^\perp(z,z^2\vec{p}_T^2)$	$154.9/176 = 0.88$
$A_{T,\mu^+\mu^-}^{\sin\phi_S}$	$\pi^- + p^\uparrow \to \mu^+\mu^- + X$	$f_{1T}^\perp(x,\vec{k}_T^2)$	$6.92/12 = 0.58$
$A_N^{W/Z}$	$p^\uparrow + p \to (W^+,W^-,Z)+X$	$f_{1T}^\perp(x,\vec{k}_T^2)$	$30.8/17 = 1.81$
A_N^π	$p^\uparrow + p \to (\pi^+,\pi^-,\pi^0)+X$	$h_1(x), F_{FT}(x,x) = \frac{1}{\pi}f_{1T}^{\perp(1)}(x), H_1^{\perp(1)}(z), \tilde{H}(z)$	$70.4/60 = 1.17$
Lattice g_T	——	$h_1(x)$	$1.82/1 = 1.82$

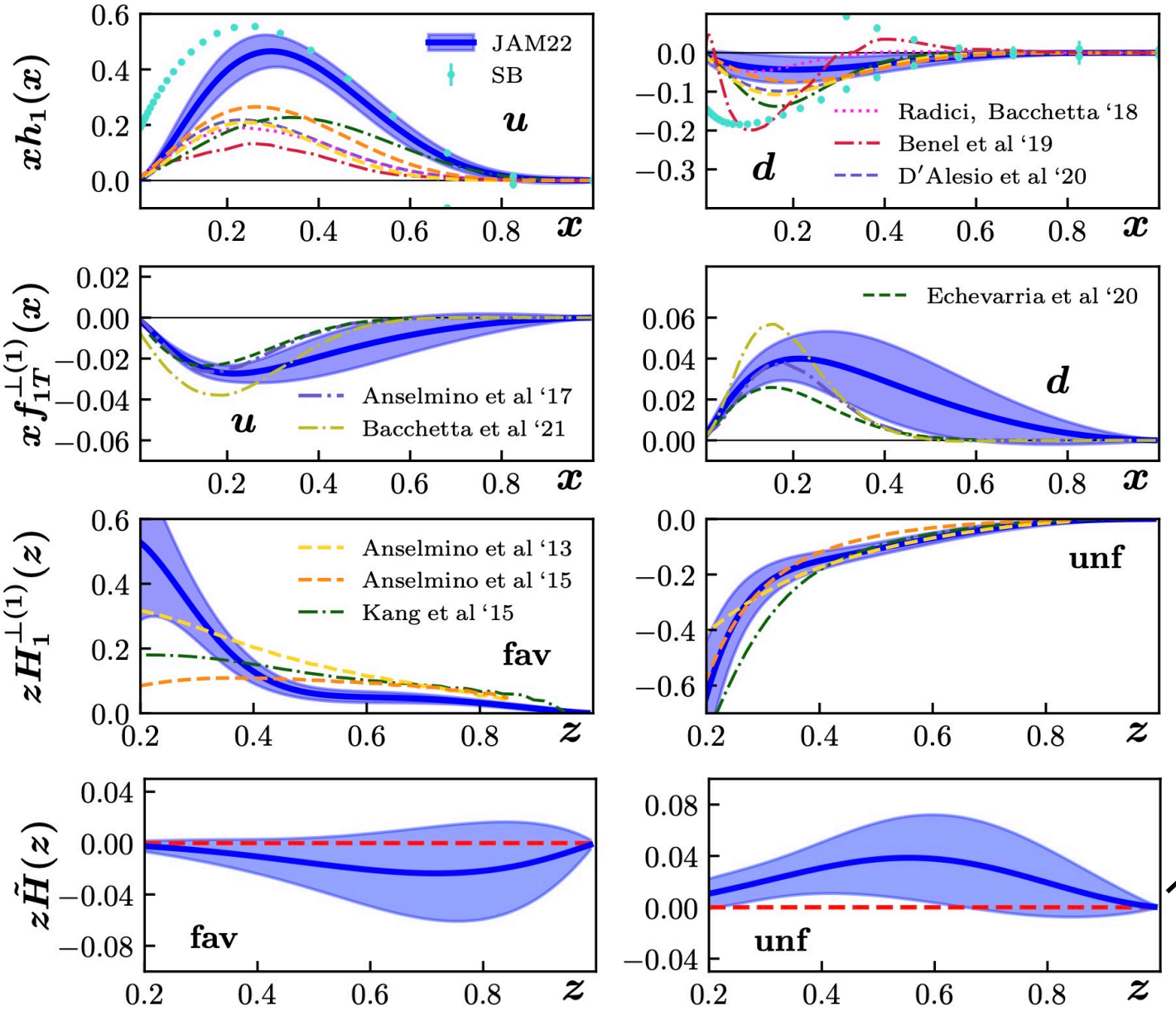

First direct information from experiment on $\tilde{H}(z)$

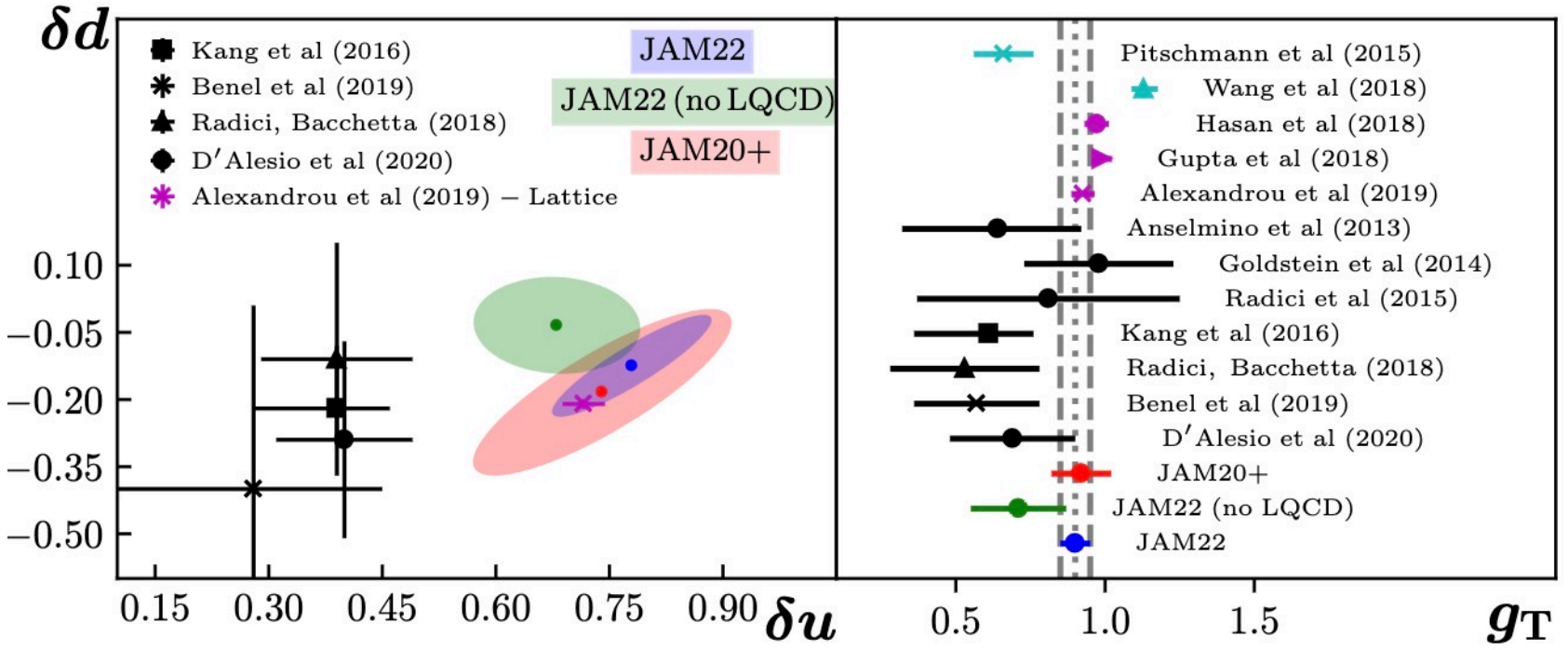

- TMD that only include e^+e^- and SIDIS Collins effect data (e.g., Kang, et al. (2016), D'Alesio, et al. (2020)) and dihadron analyses (e.g., Radici, Bacchetta (2018); Benel, Courtoy, Ferro-Hernandez (2019)), are generally below the lattice values for g_T and δu
- Note that one initially finds JAM3D-22 has more tension with lattice, but this does *not* imply phenomenology and lattice are incompatible – one can only fully answer this by including lattice data in the analysis (use it as a prior)
- **Once g_T is included (as a Bayesian prior), we find the non-perturbative functions can accommodate it *and still describe the experimental data well***

Lebanon Valley College

D. Pitonyak

QCD Global Analysis of TSSAs for Dihadron Fragmentation

DP, Cocuzza, Metz, Prokudin, Sato, Phys. Rev. Lett. **132**, 011902 (2024)

Cocuzza, Metz, DP, Prokudin, Sato, Seidl, Phys. Rev. Lett. **132**, 091901 (2024)

Cocuzza, Metz, DP, Prokudin, Sato, Seidl, Phys. Rev. D **109**, 034024 (2024)

User-friendly jupyter notebook to calculate transversity PDFs and DiFFs:
https://colab.research.google.com/github/prokudin/JAMDiFF_library/blob/main/JAMDiFF_Library.ipynb

LHAPDF tables available for transversity PDFs:
https://github.com/prokudin/JAMDiFF_library/tree/main/lhapdf

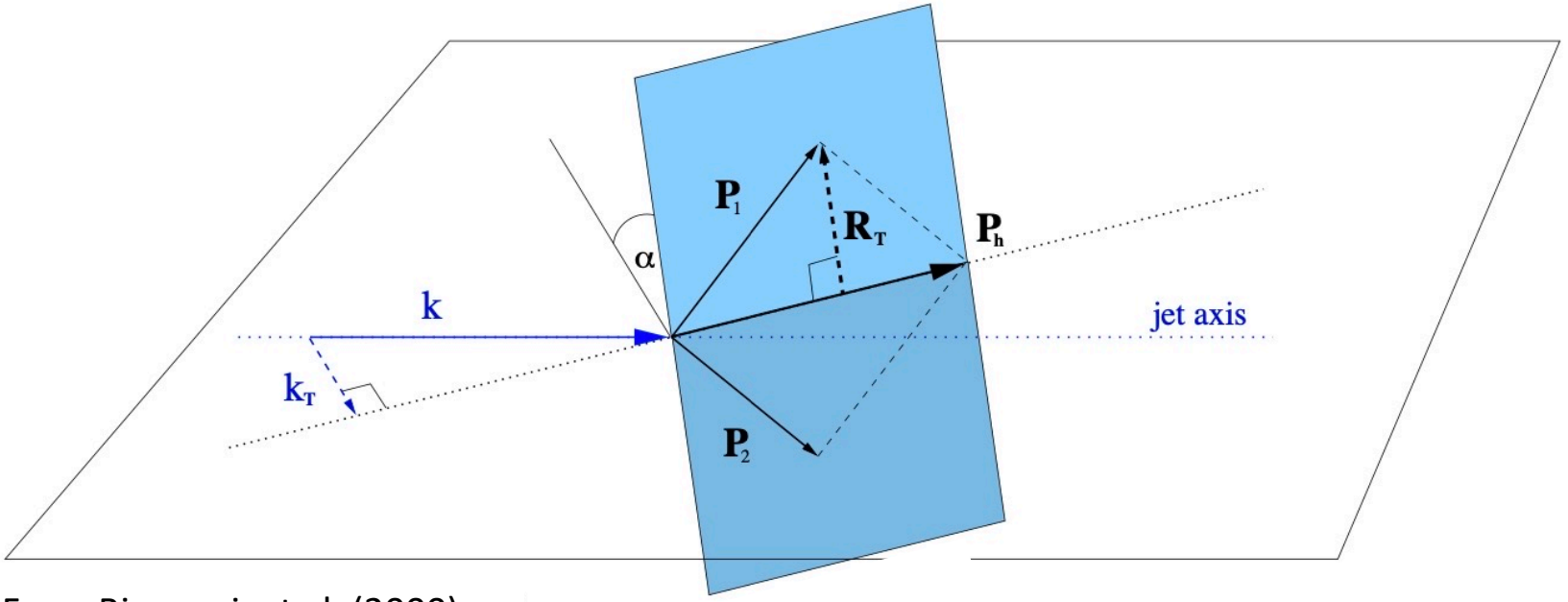

From Bianconi, et al. (2000)

Bianconi, et al. (2000); Bacchetta, Radici (2003, 2004), …

$$P_h = P_1 + P_2 \qquad R = (P_1 - P_2)/2 \qquad z = z_1 + z_2 \qquad \zeta = (z_1 - z_2)/z$$

$$P_1 = \left(\frac{M_1^2 + \vec{R}_T^2}{(1+\zeta)P_h^-}, \frac{1+\zeta}{2} P_h^-, \vec{R}_T \right) \qquad P_2 = \left(\frac{M_2^2 + \vec{R}_T^2}{(1-\zeta)P_h^-}, \frac{1-\zeta}{2} P_h^-, -\vec{R}_T \right)$$

$$\vec{R}_T^2 = \frac{1-\zeta^2}{4} M_h^2 - \frac{1-\zeta}{2} M_1^2 - \frac{1+\zeta}{2} M_2^2$$

$e^+e^- \to (h_1h_2)(\bar{h}_1\bar{h}_2)\,X$ $\quad \ell\, N^\uparrow \to \ell\,(h_1h_2)\,X$ $\quad p^\uparrow p \to (h_1h_2)\,X$

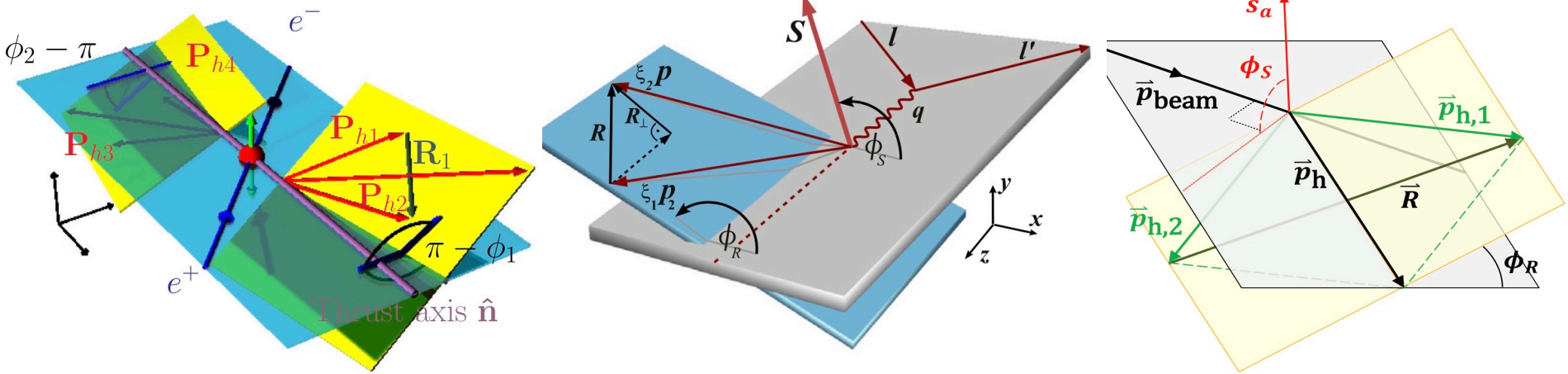

(Collins, et al. (1994); Bianconi, et al. (2000); Bacchetta, Radici (2003, 2004); Courtoy, et al. (2012); Matevosyan, et al. (2018); Radici, et al. (2013, 2015, 2018); Benel, et al. (2020), …)

$$a_{12R} = \frac{\sin^2\theta_2 \sum_q e_q^2\, H_1^{\sphericalangle,q}(z, M_h)\, H_1^{\sphericalangle,\bar{q}}(\bar{z}, \overline{M}_h)}{(1+\cos^2\theta_2)\sum_q e_q^2\, D_1^q(z, M_h)\, D_1^{\bar{q}}(\bar{z}, \overline{M}_h)}$$

Artru-Collins asymmetry

$$A_{UT}^{\sin(\phi_R+\phi_S)} = \frac{\sum_q e_q^2\, h_1^q(x)\, H_1^{\sphericalangle,q}(z, M_h)}{\sum_q e_q^2\, f_1^q(x)\, D_1^q(z, M_h)}$$

Note: D_1 can be constrained using data on $d\sigma/dz dM_h$ from BELLE (2017)

$$\frac{d\sigma}{dz\, dM_h} = \frac{4\pi N_c \alpha_{em}^2}{3Q^2} \sum_q e_q^2\, D_1^q(z, M_h)$$

$$A_{UT}^{\sin(\phi_R-\phi_S)} \sim \frac{\frac{d\Delta\hat{\sigma}_{a^\uparrow b\to c^\uparrow}}{d\hat{t}} \otimes h_1^a(x_a) \otimes f_1^b(x_b) \otimes H_1^{\sphericalangle,c}(z, M_h)}{\frac{d\hat{\sigma}_{ab\to c}}{d\hat{t}} \otimes f_1^a(x_a) \otimes f_1^b(x_b) \otimes D_1^c(z, M_h)}$$

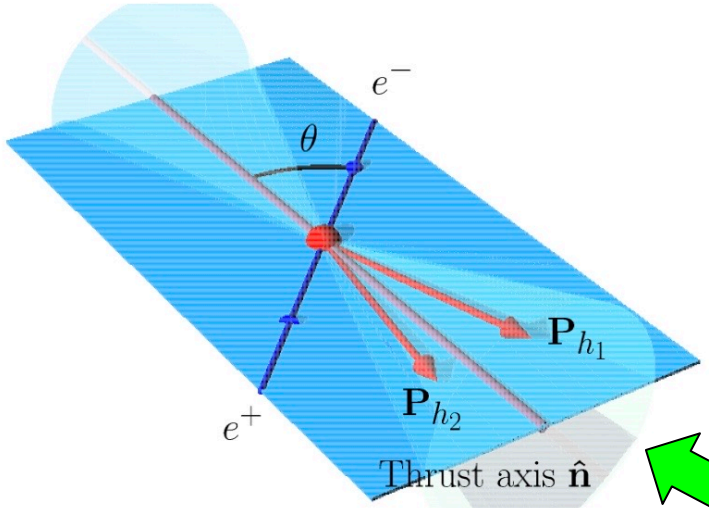

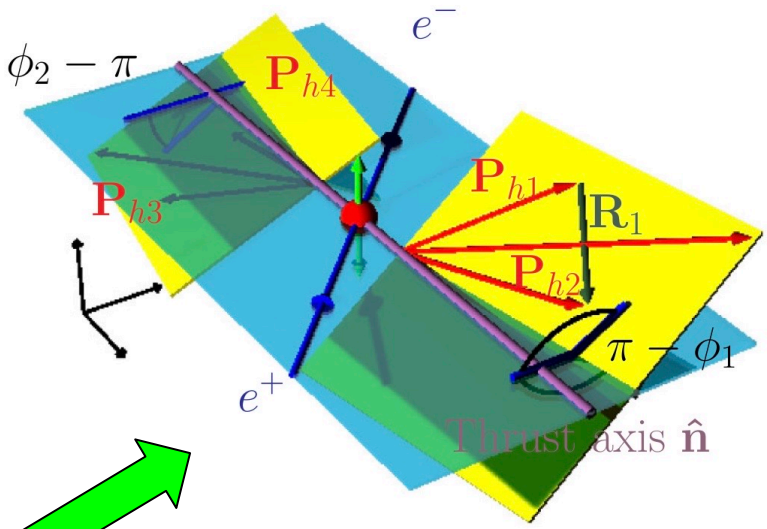

$D_1(z, M_h)$

$H_1^{\sphericalangle}(z, M_h), D_1(z, M_h)$

DiFFs and transversity PDFs extracted simultaneously

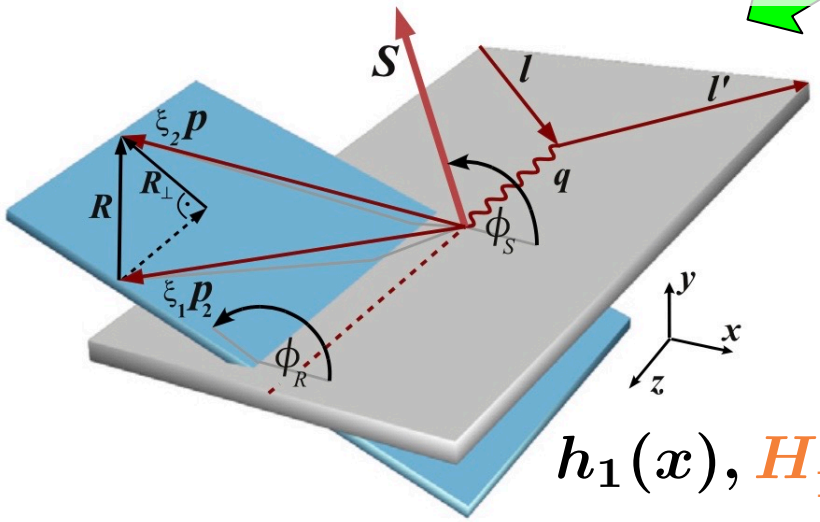

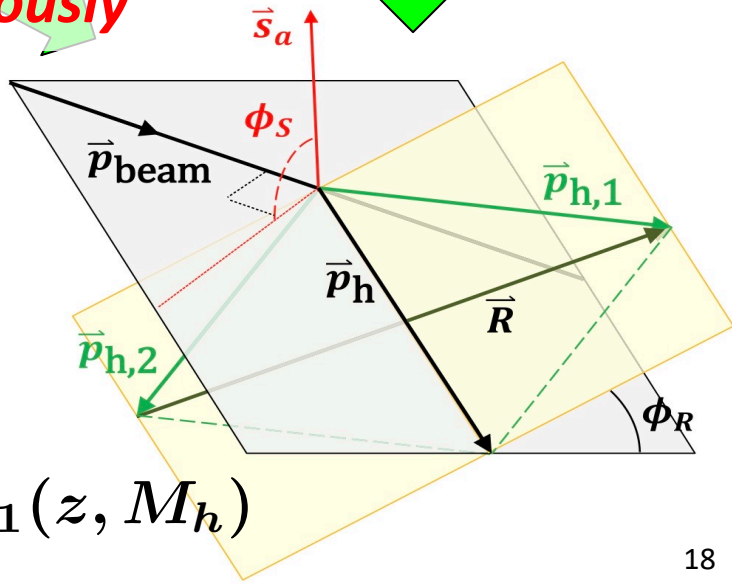

$h_1(x), H_1^{\sphericalangle}(z, M_h), D_1(z, M_h)$

- Analyze TSSAs for $\pi^+\pi^-$ production in e^+e^- annihilation, SIDIS, and proton-proton collisions and extract

$$h_1(x), H_1^{\sphericalangle}(z, M_h), D_1(z, M_h)^*$$

*Also need data from PYTHIA for flavor separation and to constrain the gluon $D_1(z,M_h)$

- We use the following functional form for the transversity PDFs u_v, d_v, and $\bar{u} = -\bar{d}$ (from large-N_c limit (Pobylitsa (2003))) and impose the Soffer bound

$$F(x) \sim N x^{\alpha}(1-x)^{\beta}(1+\gamma\sqrt{x}+\delta x)$$

Use constraint from small-x asymptotics (Kovchegov, Sievert (2019))

$$\alpha \xrightarrow{x\to 0} 1 - 2\sqrt{\frac{\alpha_s N_c}{2\pi}} \longrightarrow \alpha = 0.170 \pm 0.085$$

50% uncertainty due to unaccounted for $1/N_c$ and NLO corrections

- Analyze TSSAs for $\pi^+\pi^-$ production in e^+e^- annihilation, SIDIS, and proton-proton collisions and extract

$$\boldsymbol{h_1(x), H_1^{\sphericalangle}(z, M_h), D_1(z, M_h)^*}$$

*Also need data from PYTHIA for flavor separation and to constrain the gluon $D_1(z,M_h)$

- We use the following functional form for the transversity PDFs u_v, d_v, and $\bar{u} = -\bar{d}$ (from large-N_c limit (Pobylitsa (2003))) and impose the Soffer bound

$$F(x) \sim N x^{\alpha}(1-x)^{\beta}(1+\gamma\sqrt{x}+\delta x)$$

- The DiFFs $D_1(z, M_h), H_1^{\sphericalangle}(z, M_h)$ use the same functional form as above ($x \to z$) for the z dependence, which is repeated on a grid in M_h (more finely spaced around the resonances) and interpolated to obtain the function value at any M_h

- Perform the analysis with and without LQCD data **as a Bayesian prior** for the tensor charges $\boldsymbol{\delta u, \delta d}$ from ETMC (Alexandrou, et al. (2019)) and PNDME (Gupta, et al. (2018)) (physical pion mass and 2+1+1 flavors)

Experiment	Binning	$N_{\rm dat}$	$\chi^2_{\rm red}$ JAMDiFF (w/ LQCD)	(no LQCD)	(SIDIS only)
Belle (cross section)[64]	z, M_h	1094	1.01	1.01	1.01
Belle (Artru-Collins) [111]	z, M_h	55	1.27	1.24	1.28
	$M_h, \overline{M}_h$	64	0.60	0.60	0.60
	$z, \bar{z}$	64	0.42	0.42	0.41
HERMES [117]	$x_{\rm bj}$	4	1.77	1.70	1.67
	M_h	4	0.41	0.42	0.47
	z	4	1.20	1.17	1.13
COMPASS (p) [116]	$x_{\rm bj}$	9	1.98	0.65	0.59
	M_h	10	0.92	0.94	0.93
	z	7	0.77	0.60	0.63
COMPASS (D) [116]	$x_{\rm bj}$	9	1.37	1.42	1.22
	M_h	10	0.45	0.37	0.38
	z	7	0.50	0.46	0.46
STAR [120] $\sqrt{s} = 200$ GeV $R < 0.3$	$M_h, \eta < 0$	5	2.57	2.56	—
	$M_h, \eta > 0$	5	1.34	1.55	—
	$P_{hT}, \eta < 0$	5	0.98	1.00	—
	$P_{hT}, \eta > 0$	5	1.73	1.74	—
	η	4	0.52	1.46	—
STAR [96] $\sqrt{s} = 500$ GeV $R < 0.7$	$M_h, \eta < 0$	32	1.30	1.10	—
	$M_h, \eta > 0$	32	0.81	0.78	—
	$P_{hT}, \eta > 0$	35	1.09	1.07	—
	η	7	2.97	1.83	—
ETMC δu [77]	—	1	0.71	—	—
ETMC δd [77]	—	1	1.02	—	—
PNDME δu [71]	—	1	8.68	—	—
PNDME δd [71]	—	1	0.04	—	—
Total $\chi^2_{\rm red}$ ($N_{\rm dat}$)			**1.01** (1475)	**0.98** (1471)	0.96 (1341)

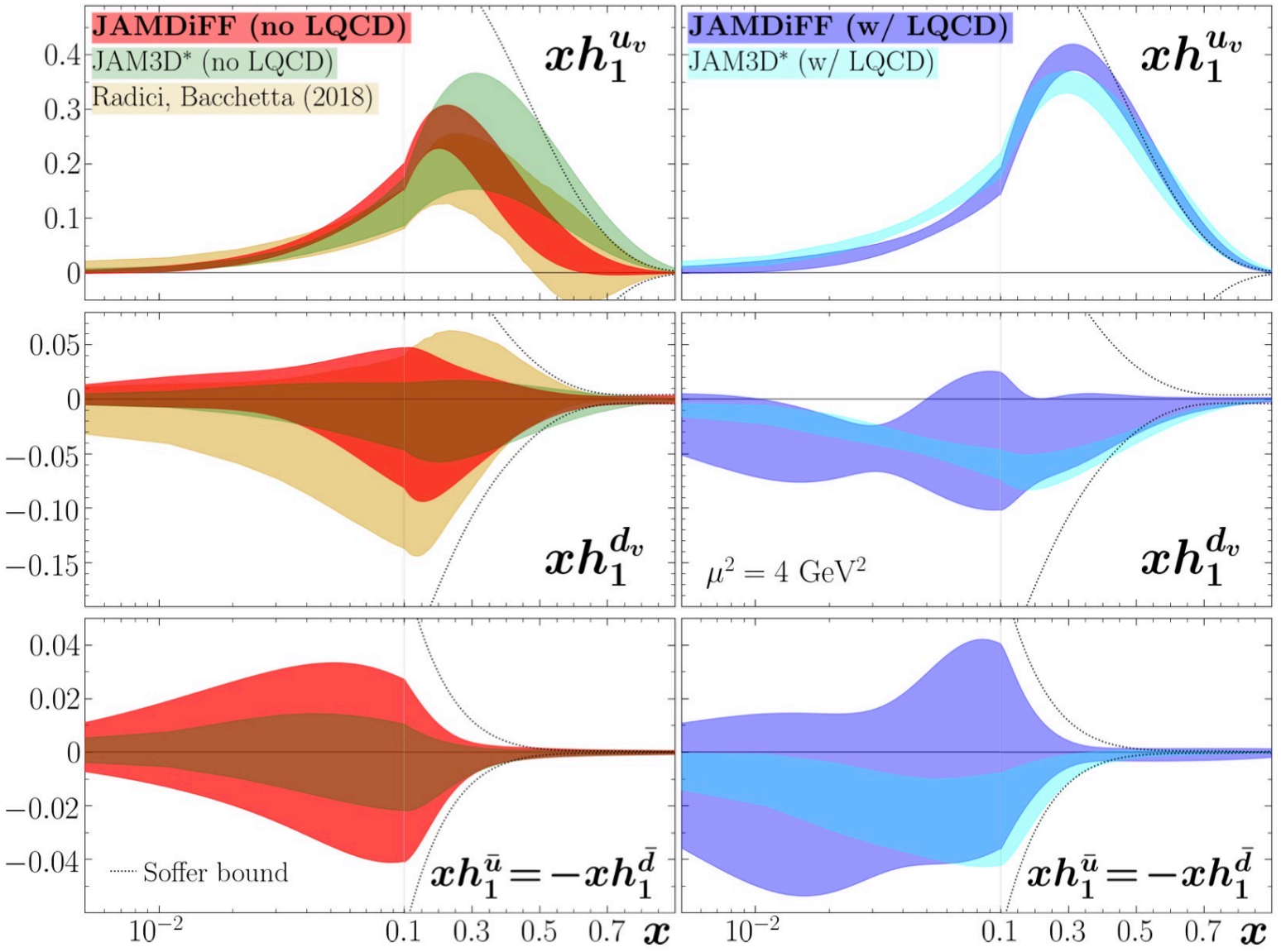

Note: JAM3D* is slightly modified from the published JAM3D-22 version: antiquarks are now included (with $\bar{u} = -\bar{d}$), $\boldsymbol{\delta u}, \boldsymbol{\delta d}$ from ETMC and PNDME are both included in the fit, and small-x constraint is imposed

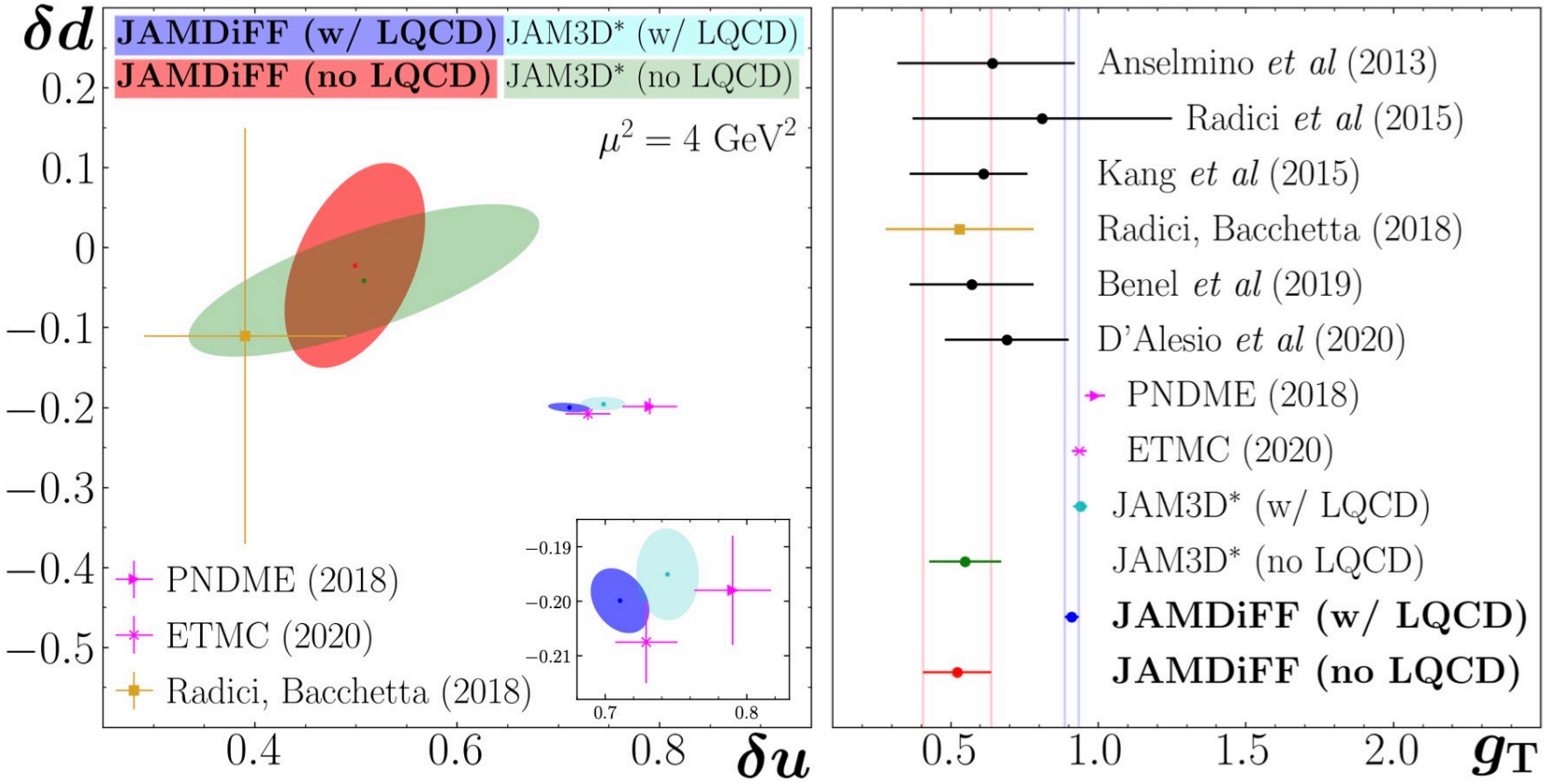

- JAMDiFF (no LQCD) agrees within errors with JAM3D* (no LQCD) and Radici, Bacchetta (2018) for the tensor charges
- Similar to the JAM3D analysis, **JAMDiFF also finds compatibility with lattice once that data is included in the fit (as a Bayesian prior),** ***and can still describe the experimental data well***

- Possible explanation for the shift (~3-4σ difference with lattice to a ~0.3-2σ difference) in the phenomenological values of the tensor charges once LQCD data is used as a prior:
  - In the no LQCD fit, h_1^{uv} has a maximum around $x \approx 0.2$ and then begins to decrease around where the x coverage of the experimental data ends ($x \approx 0.3$)
  - Within our parameterization, the PDFs fall off smoothly and monotonically as $x \rightarrow 1$, and this drives the behavior (and uncertainty) of h_1^{uv} in the unmeasured ($x > 0.3$) region
  - The fit with LQCD included has additional constraints at larger x due to the fact that one integrates from $x \in [0, 1]$ to calculate the tensor charges. This causes h_1^{uv} to now peak at slightly higher $x \approx 0.3$ in order to accommodate both LQCD and experimental data. The Soffer bound forces the with LQCD h_1^{uv} to then decrease shortly after $x = 0.35$ and the PDF again falls off smoothly and monotonically as $x \rightarrow 1$
  - **In order to further test the compatibility between LQCD and experimental data, it is of *vital importance to have more measurements at larger x (for SIDIS)* and more forward rapidity (for pp)**
  - The LQCD data and STAR $\sqrt{s}$=200 GeV data have a preference for a larger h_1^{uv} at large x, while the COMPASS proton data and STAR $\sqrt{s}$ = 500 GeV data prefer a smaller h_1^{uv}. In such a situation where there are competing preferences, and we compare analyses containing different subsets of the data, the choice of likelihood function and priors do not guarantee that the fits overlap within statistical uncertainties

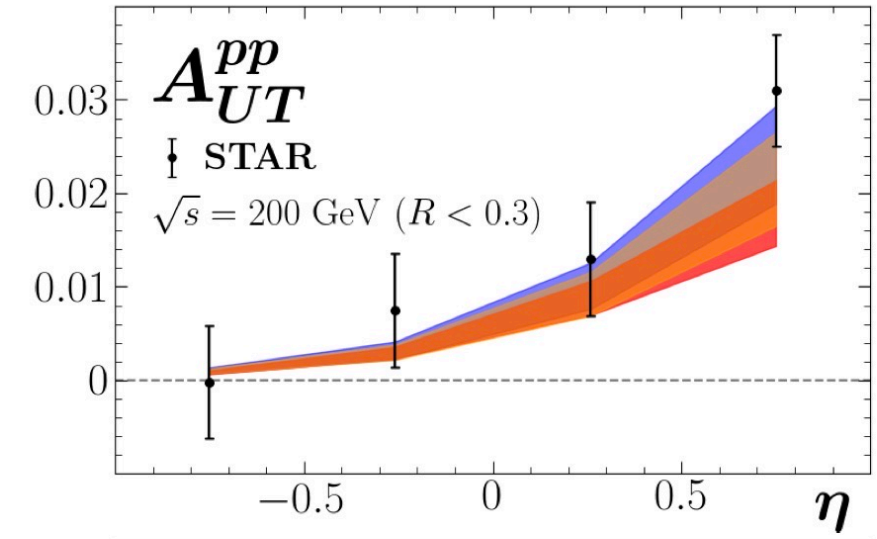
A_{UT}^{pp}
STAR
$\sqrt{s} = 200$ GeV $(R < 0.3)$
0.03
0.02
0.01
0
−0.5
0
0.5
η

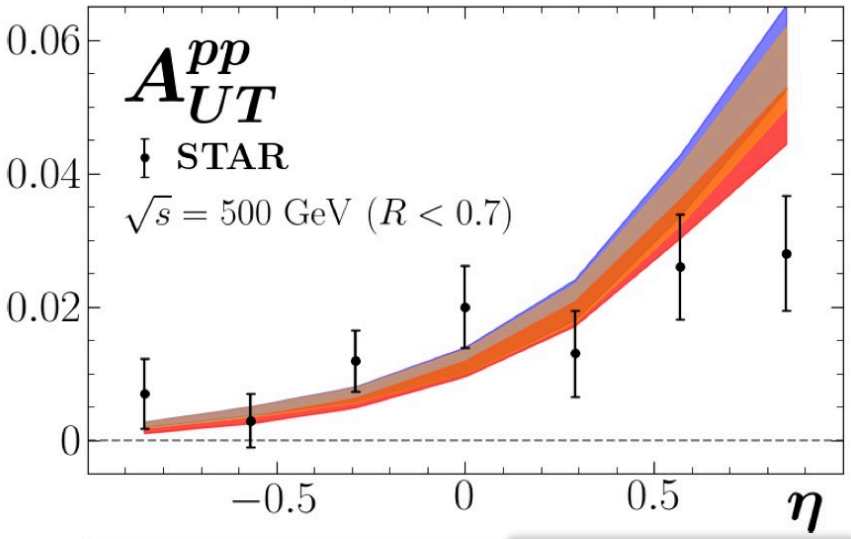
A_{UT}^{pp}
STAR
$\sqrt{s} = 500$ GeV $(R < 0.7)$
0.06
0.04
0.02
0
−0.5
0
0.5
η

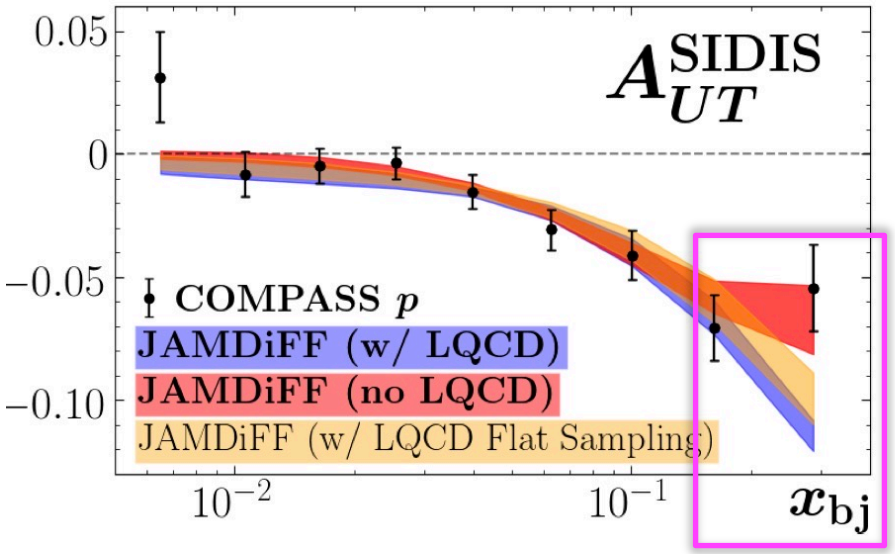
A_{UT}^{SIDIS}
0.05
0
−0.05
−0.10
COMPASS p
JAMDiFF (w/ LQCD)
JAMDiFF (no LQCD)
JAMDiFF (w/ LQCD Flat Sampling)
10^{-2}
10^{-1}
x_{bj}

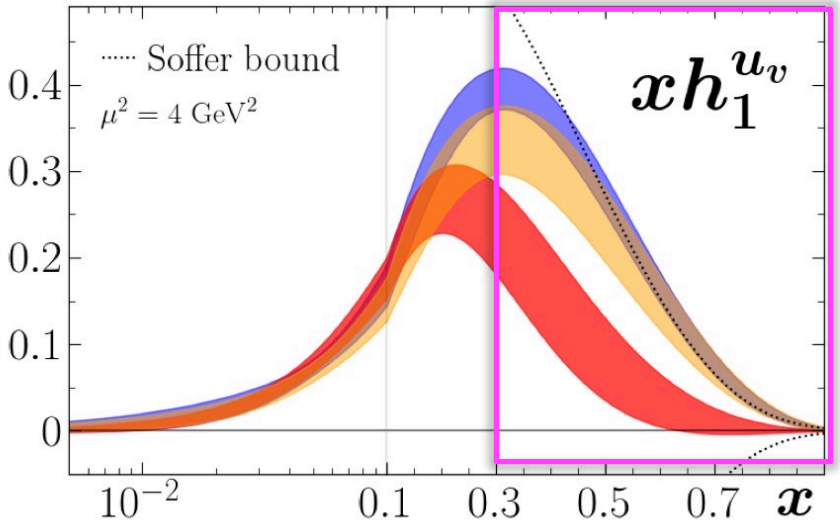
Soffer bound
$\mu^2 = 4$ GeV^2
$xh_1^{u_v}$
0.4
0.3
0.2
0.1
0
10^{-2}
0.1
0.3
0.5
0.7
x

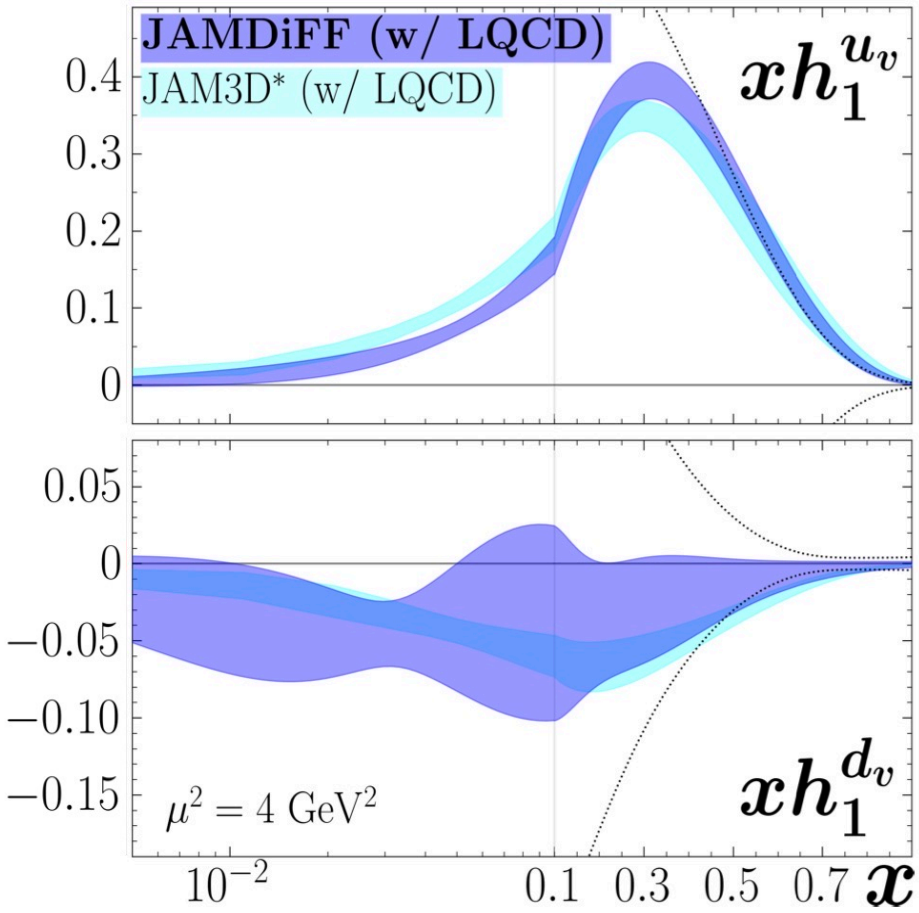

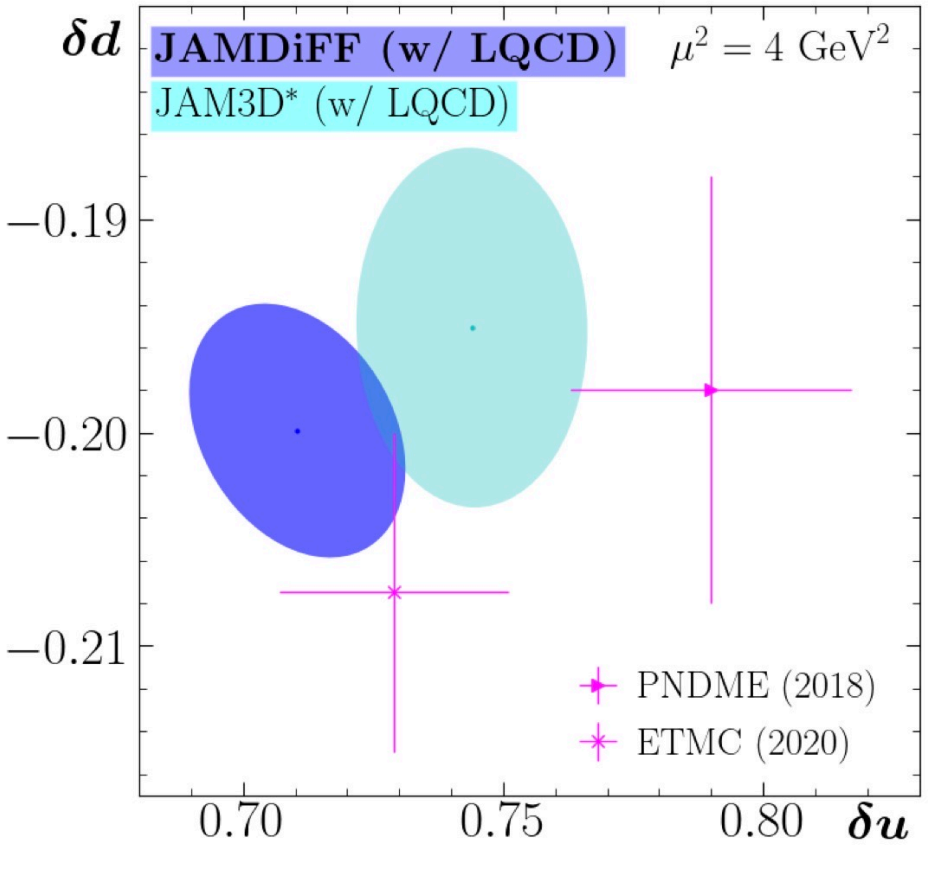

Recent analyses by the JAM Collaboration show agreement between single-hadron and dihadron approaches for extracting transversity as well as compatibility with lattice QCD tensor charges, thus demonstrating the universal nature of all this available information

Lebanon Valley College

D. Pitonyak

SoLID Impact Study on Transversity/Tensor Charge

Gamberg, Kang, DP, Prokudin, Sato, Seidl, Phys. Lett. B **816** (2021)

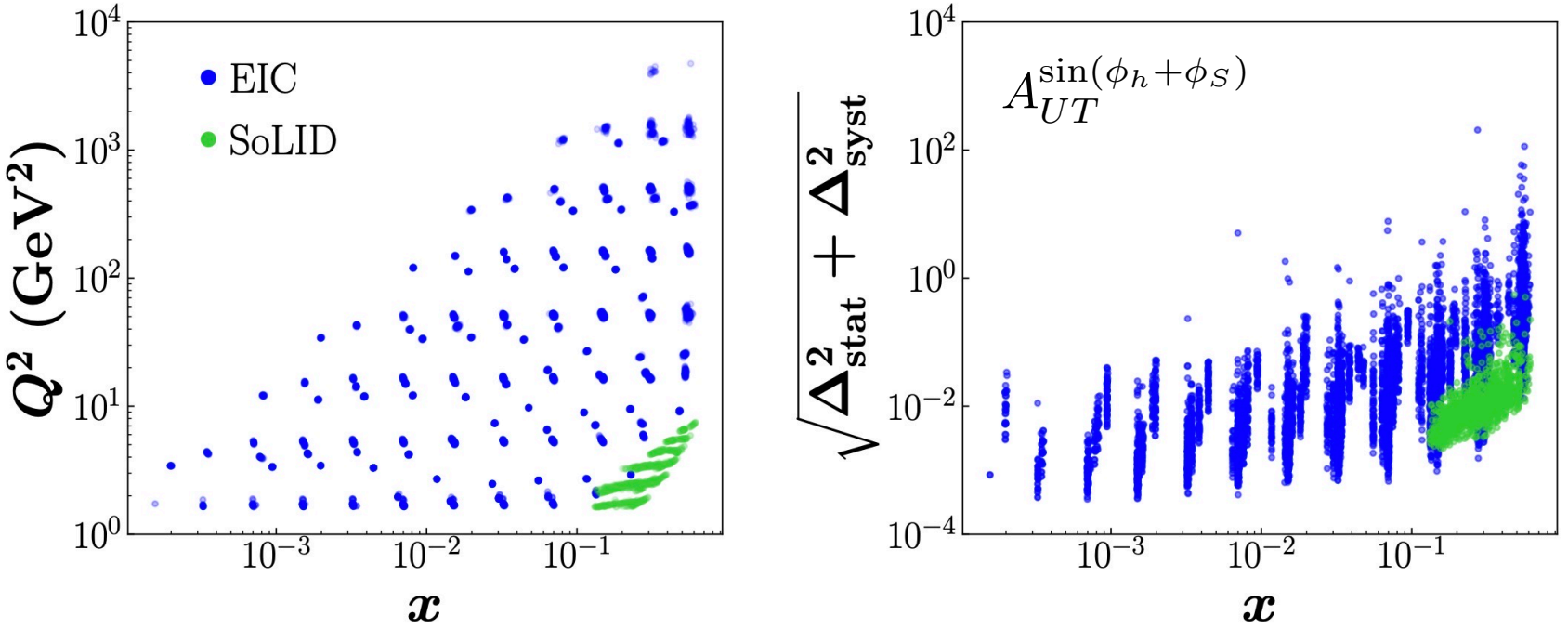

- SoLID covers a complimentary region at higher x and lower Q^2 with much greater luminosity
- Important to explore the effect of multiple measurements in different kinematic regions

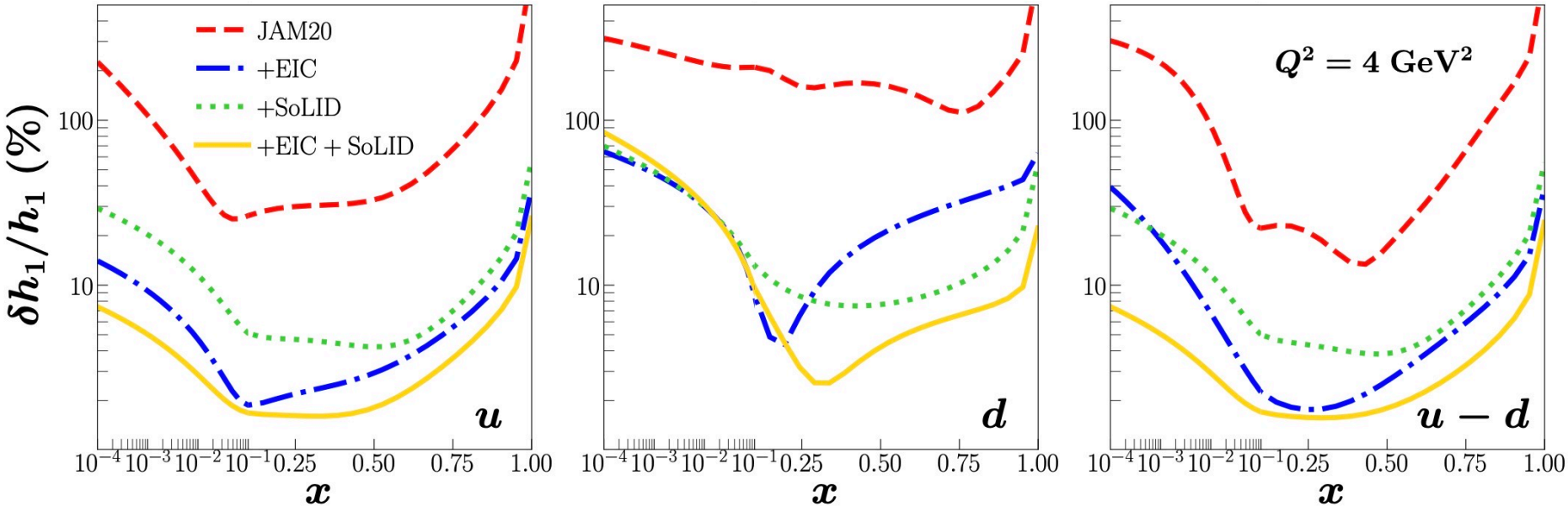

- SoLID pseudo-data was used for the Collins effect in charged pion production from both proton and He-3 targets

- SoLID reduces the relative uncertainty in $h_1^d(x)$ at higher x more than the EIC, and overall the relative uncertainties improve the most when data sets from both facilities are included

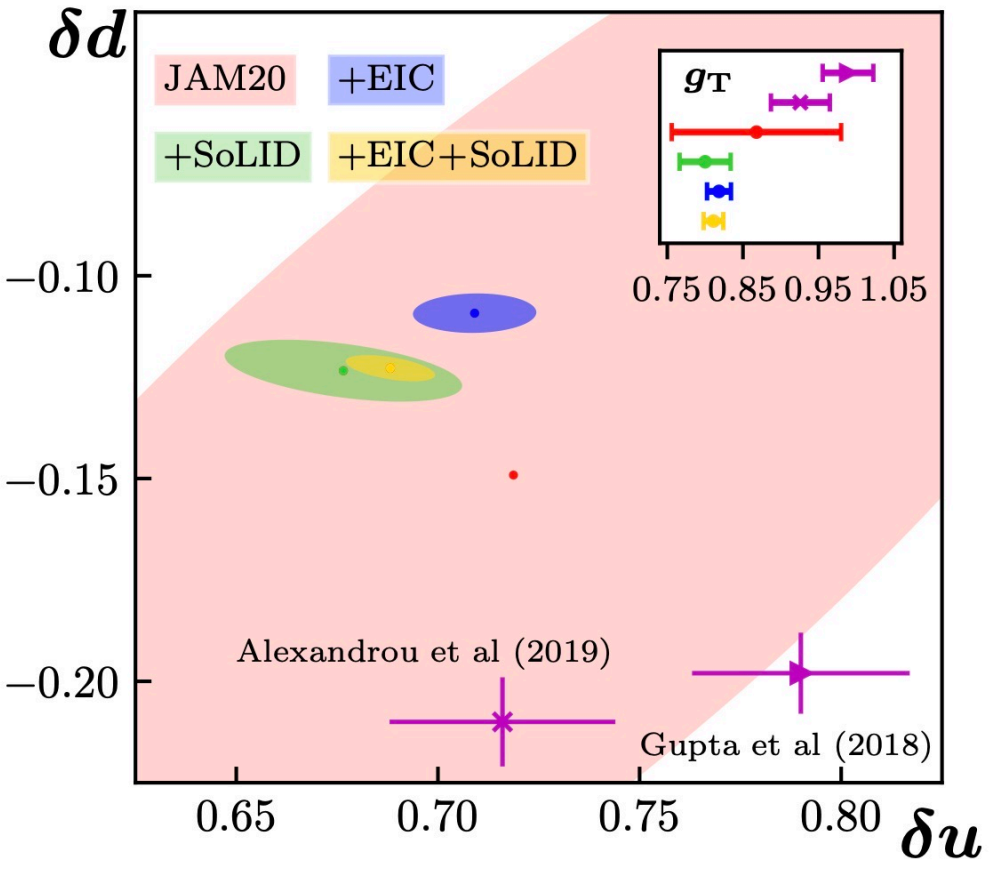

- ***Accuracy vs. precision*** – a precise measurement cannot always guarantee a very accurate extraction of the distributions, and multiple experiments, such as EIC and SoLID, should be performed in a wide kinematical region in order to minimize bias and expose any potential tensions between data sets

- The combined fit that includes both EIC and SoLID pseudo-data provides the best constraint on transversity and the tensor charges, with the results more precise than current lattice calculations

- SoLID (and EIC) data on the Collins effect (and dihadron $\sin(\phi_R + \phi_S)$) will significantly reduce the uncertainties in extractions of the transversity PDF

- Most impact will be at moderate to higher x (lower c.m. energy configurations), and ***^{3}He will play a very important role*** (more direct sensitivity to $h_1^d(x)$ and removes correlation between $\boldsymbol{\delta u}$ and $\boldsymbol{\delta d}$)

- SoLID (and EIC) data will allow phenomenological extractions of the tensor charges to become as precise as current lattice QCD calculations

Summary

- The tensor charges are fundamental properties of the nucleon that have connections to QCD phenomenology, lattice QCD and model calculations, and beyond the Standard Model studies (e.g., beta decay, EDM)

- There are two main approaches in QCD phenomenology to extract the transversity PDFs in order to compute the tensor charges: one analyzing TMD/collinear twist-3 single-hadron fragmentation observables, and the other utilizing collinear twist-2 dihadron fragmentation measurements

- Recent analyses by the JAM Collaboration (Gamberg, et al. (2022), Cocuzza, et al. (2024)) in both approaches show that lattice QCD tensor charge data currently can be accommodated within phenomenology, demonstrating the universal nature of all this available information.

- SoLID can play an important role in providing transverse-spin (single-hadron and dihadron) data, especially at moderate to larger x and with a He-3 target, that will significantly reduce the uncertainty in the extractions of $h_1(x)$ and allow us to further test the compatibility between QCD phenomenology and lattice QCD

Backup Slides

- Parameterization of the $\pi^+\pi^-$ DiFFs $\boldsymbol{D_1(z, M_h)}$, $\boldsymbol{H_1^{\sphericalangle}(z, M_h)}$

  - Symmetry relations (Courtoy, et al. (2012))

$$D_1^u = D_1^d = D_1^{\bar{u}} = D_1^{\bar{d}}, \qquad H_1^{\sphericalangle,u} = -H_1^{\sphericalangle,d} = -H_1^{\sphericalangle,\bar{u}} = H_1^{\sphericalangle,\bar{d}},$$

$$D_1^s = D_1^{\bar{s}}, \quad D_1^c = D_1^{\bar{c}}, \quad D_1^b = D_1^{\bar{b}} \qquad H_1^{\sphericalangle,s} = -H_1^{\sphericalangle,\bar{s}} = H_1^{\sphericalangle,c} = -H_1^{\sphericalangle,\bar{c}} = 0$$

also have D_1^g

  - Positivity bounds (Bacchetta, Radici (2003))

$$D_1(z, M_h) > 0 \qquad |H_1^{\sphericalangle}(z, M_h)| < D_1(z, M_h)$$

- Parameterization of the $\pi^+\pi^-$ DiFFs $\boldsymbol{D_1(z, M_h)}$, $\boldsymbol{H_1^{\sphericalangle}(z, M_h)}$
  - Because of the resonance structure of the e^+e^- cross section, we use a grid in M_h whose density depends on the flavor and DiFF and then at each grid point we have the functional form $\sim N z^a (1-z)^b$. The grid is then interpolated to give a general M_h dependence. E.g., for the up quark for D_1,

$$\mathbf{M}_h^u = [2m_\pi, 0.40, 0.50, 0.70, 0.75, 0.80, 0.90, 1.00, 1.20, 1.30, 1.40, 1.60, 1.80, 2.00] \text{ GeV}$$

$$D_1^u(z, \mathbf{M}_h^{u,i}) = \sum_{j=1,2,3} \frac{N_{ij}^u z^{\alpha_{ij}^u} (1-z)^{\beta_{ij}^u}}{\mathrm{B}[\alpha_{ij}^u + 1, \beta_{ij}^u + 1]}$$

$\rightarrow$ 204 parameters for D_1 and 48 parameters for $H_1^{\sphericalangle}$

- Parameterization of the $\pi^+\pi^-$ DiFFs $\boldsymbol{D_1(z, M_h)}$, $\boldsymbol{H_1^{\sphericalangle}(z, M_h)}$

  - Because of the resonance structure of the e^+e^- cross section, we use a grid in M_h whose density depends on the flavor and DiFF and then at each grid point we have the functional form $\sim N z^a (1-z)^b$. The grid is then interpolated to give a general M_h dependence. E.g., for the up quark for D_1,

$$\mathbf{M}_h^u = [2m_\pi, 0.40, 0.50, 0.70, 0.75, 0.80, 0.90, 1.00, 1.20, 1.30, 1.40, 1.60, 1.80, 2.00] \text{ GeV}$$

$$D_1^u(z, \mathbf{M}_h^{u,i}) = \sum_{j=1,2,3} \frac{N_{ij}^u z^{\alpha_{ij}^u} (1-z)^{\beta_{ij}^u}}{\mathrm{B}[\alpha_{ij}^u + 1, \beta_{ij}^u + 1]}$$

$\rightarrow$ 204 parameters for D_1 and 48 parameters for $H_1^{\sphericalangle}$

  - The Belle data is not sufficient to perform a flavor separation for D_1, so we supplement with data from Pythia for σ^q/σ^{tot} for $q = s, c, b$ at

$\sqrt{s} = [10.58, 30.73, 50.88, 71.04, 91.19]$ GeV

using different tunes to quantify systematic uncertainties

$\rightarrow$ constrain D_1 for s, c, b as well as the gluon through scaling violations

- Remark about χ^2 definition and Bayesian priors

$$\mathcal{P}(\boldsymbol{a}|\text{data}) \propto \mathcal{L}(\boldsymbol{a}, \text{data})\,\pi(\boldsymbol{a}) \qquad \mathcal{L}(\boldsymbol{a}, \text{data}) = \exp\left(-\frac{1}{2}\chi^2(\boldsymbol{a}, \text{data})\right)$$

$$\chi^2(\boldsymbol{a}) = \sum_{e,i}\left(\frac{d_{e,i} - \sum_k r_{e,k}\beta^k_{e,i} - T_{e,i}(\boldsymbol{a})/N_e}{\alpha_{e,i}}\right)^2$$

Only experimental data included in the χ^2 function (no LQCD)

$$\pi(\boldsymbol{a}) = \prod_l \Theta\left((a_l - a_l^{\min})(a_l^{\max} - a_l)\right) \prod_f \prod_i \exp\left\{-\frac{1}{2}\left(\frac{d_{f,i} - T_{f,i}(\boldsymbol{a})}{\alpha_{f,i}}\right)^2\right\}$$

$$\times \prod_e \prod_k \exp\left\{-\frac{1}{2}r^2_{e,k}\right\} \prod_e \exp\left\{-\frac{1}{2}\left(\frac{1 - N_e}{\delta N_e}\right)^2\right\} \exp\left\{-\frac{1}{2}\Delta^2_{D_1<0}\right\} \exp\left\{-\frac{1}{2}\Delta^2_{|H_1^<|>D_1}\right\} \exp\left\{-\frac{1}{2}\Delta^2_{\text{SB}}\right\}$$

LQCD data included as a prior

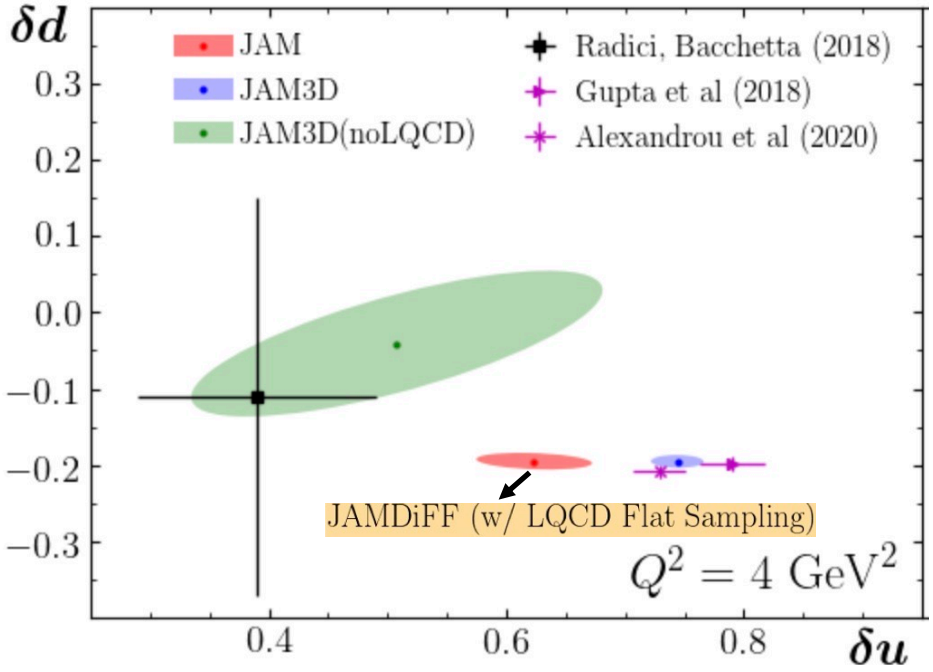
δd
JAM
JAM3D
JAM3D(noLQCD)
Radici, Bacchetta (2018)
Gupta et al (2018)
Alexandrou et al (2020)
0.3
0.2
0.1
0.0
−0.1
−0.2
−0.3
JAMDiFF (w/ LQCD Flat Sampling)
$Q^2 = 4$ GeV^2
0.4
0.6
0.8
δu

Gamberg, Kang, DP, Prokudin, Sato, Seidl, PLB **816** (2021)

EIC Pseudo-data			
Observable	**Reactions**	**CM Energy ($\sqrt{S}$)**	**$N_{\text{pts.}}$**
Collins (SIDIS)	$e + p^{\uparrow} \to e + \pi^{\pm} + X$	141 GeV	756 (π^+) 744 (π^-)
		63 GeV	634 (π^+) 619 (π^-)
		45 GeV	537 (π^+) 556 (π^-)
		29 GeV	464 (π^+) 453 (π^-)
	$e + {}^3He^{\uparrow} \to e + \pi^{\pm} + X$	85 GeV	647 (π^+) 650 (π^-)
		63 GeV	622 (π^+) 621 (π^-)
		29 GeV	461 (π^+) 459 (π^-)
		Total EIC $N_{\text{pts.}}$	**8223**

Assumed accumulated luminosities of 10 fb^{-1}, 70% polarization, conservatively accounted for detector smearing and acceptance effects

Gamberg, Kang, DP, Prokudin, Sato, Seidl, PLB **816** (2021)

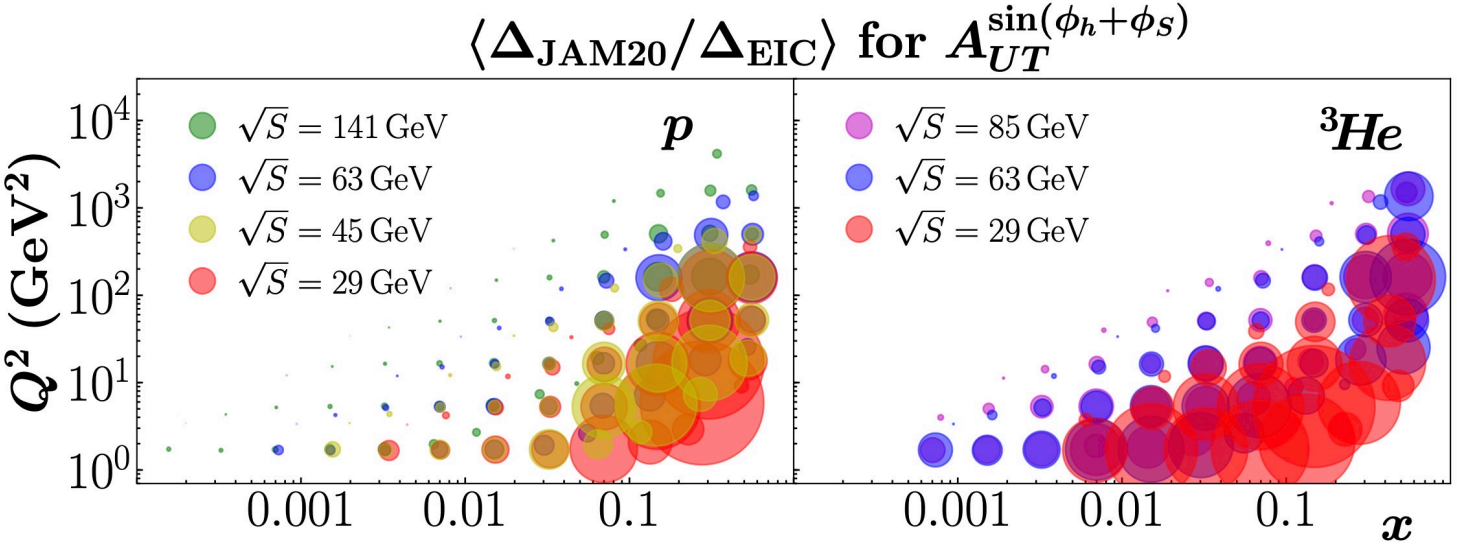

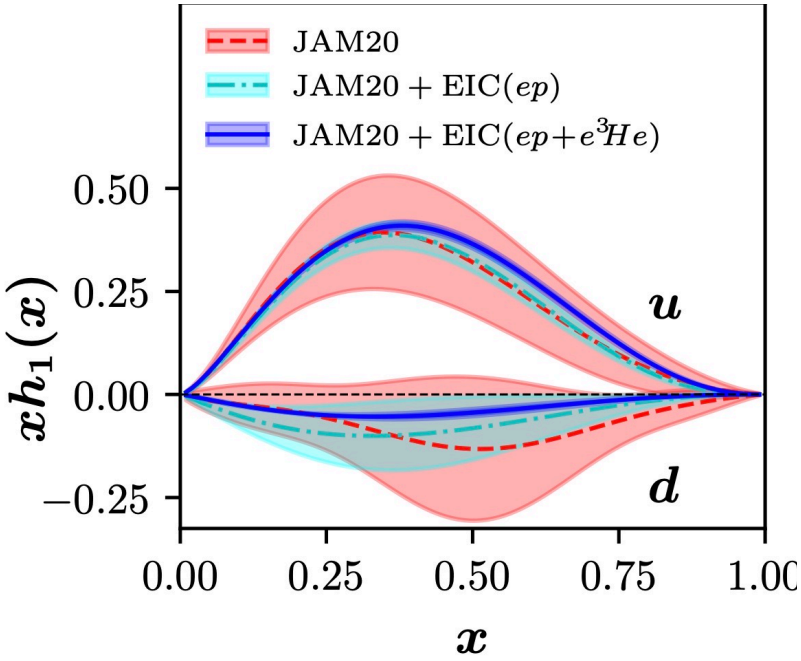

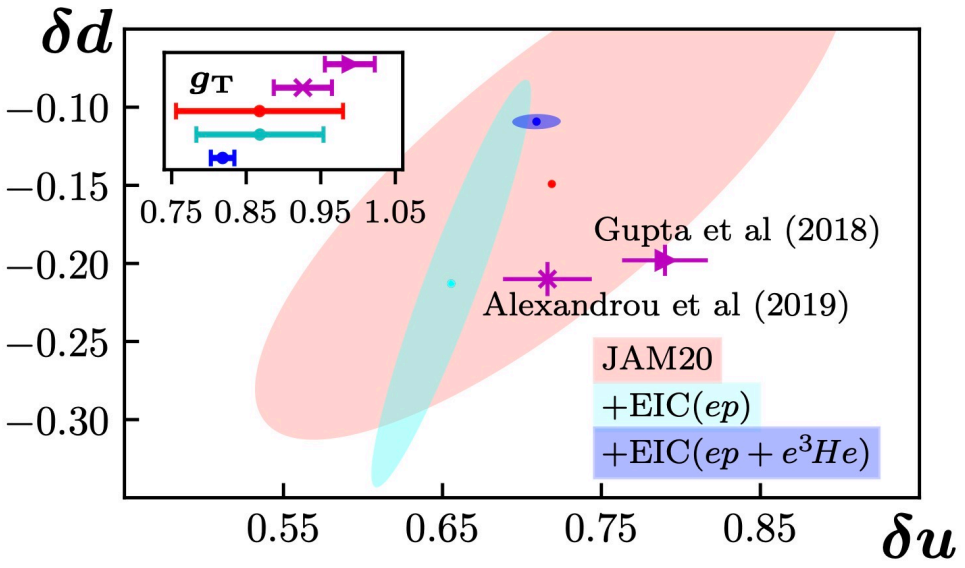

$$D_1^{h_1 h_2/q}(z,\zeta,\vec{k}_T^2,\vec{R}_T^2,\vec{k}_T\cdot\vec{R}_T) = \frac{z}{32\pi^3(1-\zeta^2)}\mathrm{Tr}\left[\Delta^{h_1 h_2/q}(z,\vec{k}_T;P_1,P_2)\gamma^-\right]$$

$$D_1^{h_1 h_2/q}(z, \zeta, \vec{k}_T^2, \vec{R}_T^2, \vec{k}_T \cdot \vec{R}_T) = \frac{z}{32\pi^3(1-\zeta^2)} \mathrm{Tr}\left[\Delta^{h_1 h_2/q}(z, \vec{k}_T; P_1, P_2)\gamma^-\right]$$

$$\sum_{h_1}\sum_{h_2} \int dz\, d\zeta\, d^2\vec{k}_T\, d^2\vec{R}_T\, D_1^{h_1 h_2/q}(z, \zeta, \vec{k}_T^2, \vec{R}_T^2, \vec{k}_T \cdot \vec{R}_T) = \underbrace{\langle \mathcal{N}(\mathcal{N}-1) \rangle}$$

Expectation value for the total number of *hadron pairs* produced when the parton fragments

Note: Recent papers by Collins, Rogers (2024) and Rogers, Courtoy (2024) do *not* actually put into question our results.

$$D_1^{h_1 h_2/q}(z,\zeta,\vec{k}_T^{\,2},\vec{R}_T^{\,2},\vec{k}_T\cdot\vec{R}_T) = \frac{z}{32\pi^3(1-\zeta^2)}\,\mathrm{Tr}\left[\Delta^{h_1 h_2/q}(z,\vec{k}_T;P_1,P_2)\gamma^-\right]$$

$$\sum_{h_1}\sum_{h_2}\int dz\, d\zeta\, d^2\vec{k}_T\, d^2\vec{R}_T\, D_1^{h_1 h_2/q}(z,\zeta,\vec{k}_T^{\,2},\vec{R}_T^{\,2},\vec{k}_T\cdot\vec{R}_T) = \underbrace{\langle \mathcal{N}(\mathcal{N}-1)\rangle}$$

Expectation value for the total number of *hadron pairs* produced when the parton fragments

Note: Recent papers by Collins, Rogers (2024) and Rogers, Courtoy (2024) do *not* actually put into question our results.

$$e^+e^- \to (h_1 h_2)\, X$$

$$\frac{d\sigma}{dz\, d\zeta d^2\vec{R}_T} = \sum_q \boxed{\frac{4\pi N_c \alpha_{\rm em}^2}{3Q^2}\, e_q^2}\, D_1^{h_1 h_2/q}(z,\zeta,\vec{R}_T^{\,2})$$

total partonic cross section for $e^+e^- \to \gamma \to q\bar{q} \equiv \hat{\sigma}_0^q$

$$D_1^{h_1 h_2/q}(z,\zeta,\vec{k}_T^{\,2},\vec{R}_T^{\,2},\vec{k}_T\cdot\vec{R}_T) = \frac{z}{32\pi^3(1-\zeta^2)}\,\mathrm{Tr}\left[\Delta^{h_1 h_2/q}(z,\vec{k}_T;P_1,P_2)\gamma^-\right]$$

$$\sum_{h_1}\sum_{h_2}\int dz\,d\zeta\,d^2\vec{k}_T\,d^2\vec{R}_T\,D_1^{h_1 h_2/q}(z,\zeta,\vec{k}_T^{\,2},\vec{R}_T^{\,2},\vec{k}_T\cdot\vec{R}_T) = \underbrace{\langle \mathcal{N}(\mathcal{N}-1)\rangle}$$

Expectation value for the total number of *hadron pairs* produced when the parton fragments

Note: Recent papers by Collins, Rogers (2024) and Rogers, Courtoy (2024) do *not* actually put into question our results.

$$e^+e^- \to (h_1 h_2)\,X$$

$$\frac{d\sigma}{dz\,d\zeta d^2\vec{R}_T} = \sum_q \boxed{\frac{4\pi N_c \alpha_{\rm em}^2}{3Q^2}\,e_q^2}\,D_1^{h_1 h_2/q}(z,\zeta,\vec{R}_T^{\,2})$$

total partonic cross section for $e^+e^- \to \gamma \to q\bar{q} \equiv \hat{\sigma}_0^q$

$$e^+e^- \to h\,X$$

$$\frac{d\sigma}{dz} = \sum_q \hat{\sigma}_0^q\,D_1^{h/q}(z)$$

$$D_1^{h_1 h_2/q}(z,\zeta,\vec{k}_T^2,\vec{R}_T^2,\vec{k}_T\cdot\vec{R}_T) = \frac{z}{32\pi^3(1-\zeta^2)}\mathrm{Tr}\left[\Delta^{h_1 h_2/q}(z,\vec{k}_T;P_1,P_2)\gamma^-\right]$$

$$\sum_{h_1}\sum_{h_2}\int dz\, d\zeta\, d^2\vec{k}_T\, d^2\vec{R}_T\, D_1^{h_1 h_2/q}(z,\zeta,\vec{k}_T^2,\vec{R}_T^2,\vec{k}_T\cdot\vec{R}_T) = \underbrace{\langle \mathcal{N}(\mathcal{N}-1)\rangle}$$

Expectation value for the total number of *hadron pairs* produced when the parton fragments

Note: Recent papers by Collins, Rogers (2024) and Rogers, Courtoy (2024) do *not* actually put into question our results.

$e^+e^- \to (h_1 h_2)\, X$

$$\frac{d\sigma}{dz\, d\zeta d^2\vec{R}_T} = \sum_q \boxed{\frac{4\pi N_c \alpha_{\rm em}^2}{3Q^2}\, e_q^2}\, D_1^{h_1 h_2/q}(z,\zeta,\vec{R}_T^2)$$

total partonic cross section for $e^+e^- \to \gamma \to q\bar{q} \equiv \hat{\sigma}_0^q$

$e^+e^- \to h\, X$

$$\frac{d\sigma}{dz} = \sum_q \hat{\sigma}_0^q\, D_1^{h/q}(z)$$

$$\boldsymbol{D_1^{h_1 h_2/i}(w,x,\vec{Y}^2,\vec{Z}^2,\vec{Y}\cdot\vec{Z}) \equiv \mathcal{J}\cdot D_1^{h_1 h_2/i}(z,\zeta,\vec{k}_T^2,\vec{R}_T^2,\vec{k}_T\cdot\vec{R}_T)}$$

is a number density

Jacobian for the variable transformation

DiFFs extracted from experiment now have a clear physical meaning:

they are densities in the momentum variables for the number of hadron pairs $(h_1 h_2)$ fragmenting from the parton